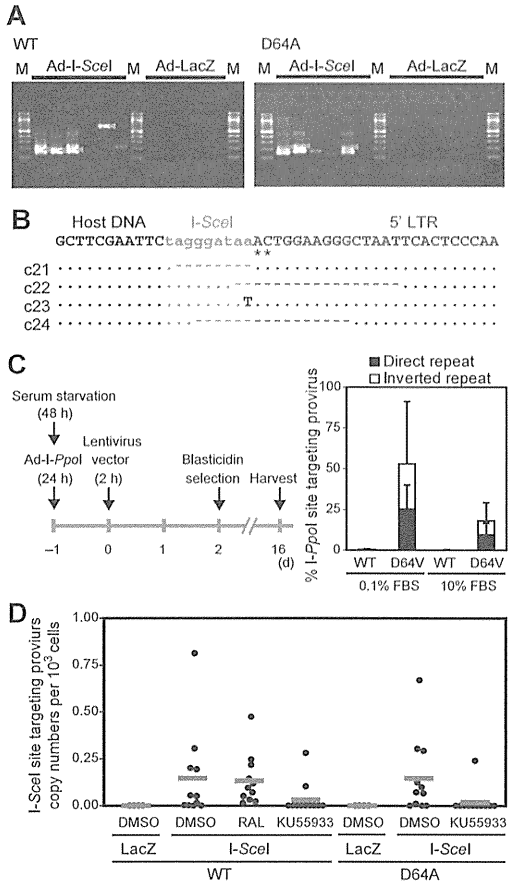

Figure 2 Frequent integration of the IN-CA defective virus into the DSB site. (**A**) PCR amplification of provirus DNA integrated into the I-*Sce*I site after infection of WT virus (left) or NL-Luc-IN-D64A-E(−)R(−) virus (D64A virus) (right). PMA-treated THP-1/I-*Sce*I cells were used. Each lane shows an independent result that was obtained from cells cultured in a single well of 6-multiwell. For each test group, six wells were independently infected with viruses. M, molecular marker. Arrowheads indicate amplicons of viral DNA integrated in the I-*Sce*I site, which was further confirmed by sequence analysis. (**B**) Sequence data of D64A provirus DNA that was integrated in the I-*Sce*I site. A representative result is shown at the top. Asterisks indicate the pAC. Dots indicate identical nucleotides to those of the representative sequence. Dashes indicate deleted nucleotides. (**C**) Experimental protocol for evaluating the frequency of viral integration into the DSB site. I-*Ppo*I-qPCR and EGFP-qPCR analyses were done for quantification of I-*Ppo*I site-specific and total proviral DNA copy numbers, respectively. Representative data of two independent experiments was shown. Error bars, s.d. of triplicate assays. (**D**) Evaluation of I-*Sce*I site-targeting efficiency. PMA-treated THP-1/I-*Sce*I cells were infected with WT or D64A virus for 2 h, and cells were harvested 48 hpi for the I-*Sce*I-qPCR analysis (see Methods section). To cleave the I-*Sce*I site, cells were infected with the Ad-I-*Sce*I at an MOI of 100 from 1 h post HIV-1 infection. Treatment with RAL and KU55933 was conducted from −2 h to 48 hpi. Effects of RAL and KU55933 were evaluated on 11 samples that were prepared from three independent experiments. Each dot indicates copy numbers of provirus DNA that had integrated in the I-*Sce*I site in 10^3 cells, which were infected as a single test sample.

10% and 0.1% FBS, respectively (Additional file 1, Figure S3B). The data indicated that the cellular conditions had a large influence on the rate of viral integration into DSB sites. Of note, no remarkable integration of WT virus into the DSB site was detected under any conditions of cell culture with different concentrations of FBS (Figure 2C). These data suggested that the IN-CA–defective virus was the main target of capture by the DSB sites.

To accurately determine the exact rate of DSB-specific integration of viral DNA, we developed a system for quantitative I-*Sce*I-PCR (I-*Sce*I-qPCR) analysis of the provirus DNA and investigated whether viral DNA integration into the I-*Sce*I site was influenced by RAL (see experimental procedures in Methods section). As shown in Figure 2D, RAL did not attenuate the DSB-specific integration of WT viruses in PMA-treated THP-1 cells (a single dot indicates each result of 11 samples in three independent experimental groups). In contrast, KU55933 efficiently blocked the DSB-specific integration of WT and D64A viruses (Figure 2D). These data suggest that capture of viral DNA in the DSB sites was selectively induced in an IN-CA–independent manner, which was ATM-dependent.

DNA damaging agents upregulate IN-CA–independent viral integration

Next, we examined the effects of the DNA damaging agents etoposide and bleomycin on viral infection. As shown in Figure 3A, both compounds increased the infectivity of D64A virus in all cells examined, which included MDMs and various human cell lines. However, the positive effects of these compounds were not consistently observed in WT virus, although they ectopically enhanced the frequency of viral transduction (Figure 3B, Additional file 1, Figure S4), i.e., etoposide enhanced the infectivity of WT virus in serum-starved HT1080 cells and nocodazole-treated human primary fibroblasts (TIG-3) (Figure 3B, upper panels, Additional file 1, Figure S4) [24]. However, it had no positive effects when cells were cultured in the presence of 10% FBS (Figure 3B, upper panels, Additional file 1, Figure S4). In addition, bleomycin had no positive effects on the infectivity of WT virus under any culture conditions (Figure 3B, lower panels, Additional file 1, Figure S4). These data indicate that the effects of DNA damage on viral transduction are only observable when combined with the IN-CA–defective virus, or they are obscured by the infectivity of the WT virus.

DSBs enhanced viral transduction at the integration step of viral infection

We quantified the integrated DNA copy numbers to clarify the roles of DSBs in IN-CA–independent viral transduction in greater detail. We used serum-starved HT1080 cells to minimize the possible effects of DSBs generated

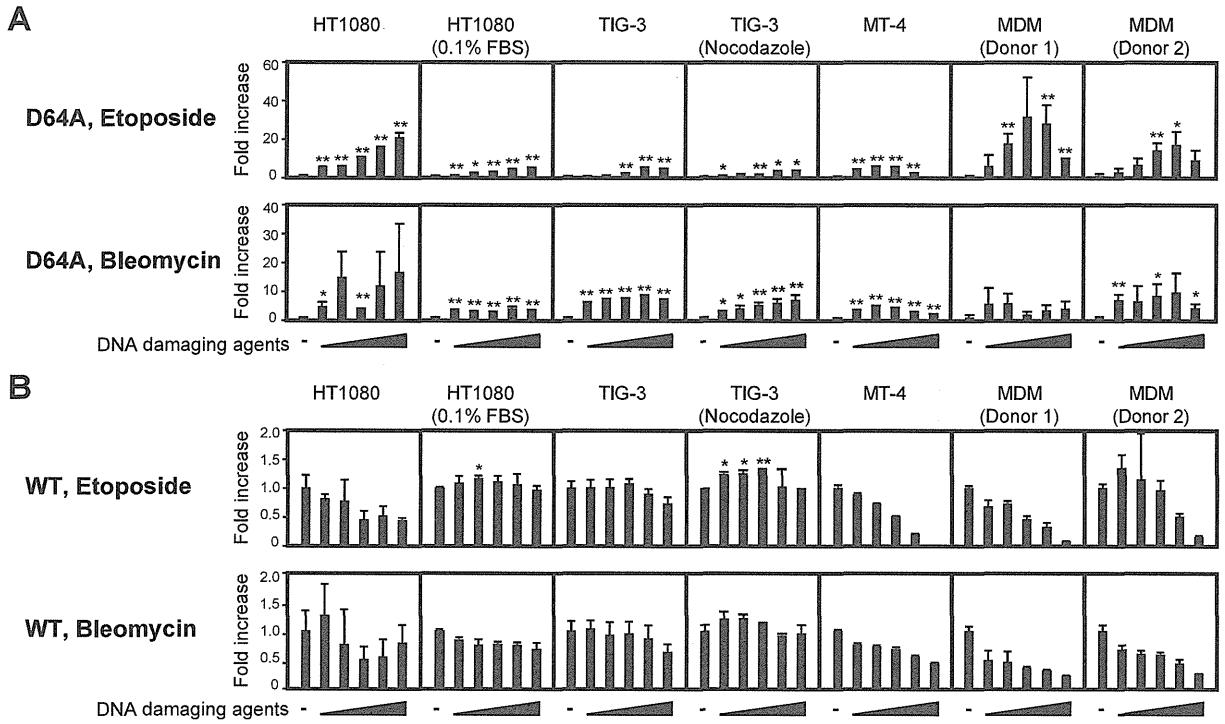

Figure 3 DNA damage enhances the IN-CA independent infectivity of HIV-1. Cells were infected with D64A (**A**) or WT (**B**) viruses in the presence of etoposide or bleomycin from 0–48 h post-infection (hpi). After 48 h, cell extracts were prepared and subjected to the luciferase assay. The fold increase of the activity after each viral infection with or without DNA damaging agents was shown. In experiments using cell lines, representative data from one of repeated experiments was shown. Results are presented as mean ± s.d. of triplicate assays. All cells except for MT-4 cells were treated with 0, 0.625, 1.25, 2.5, 5, 10 μM etoposide or 0, 1.25, 2.5, 5, 10, 20 μM bleomycin. MT-4 cells were treated with 0, 0.039, 0.078, 0.156, 0.313, 0.625 μM etoposide or 0, 0.078, 0.156, 0.313, 0.625, 1.25 μM bleomycin. Raw data of luciferase activity was shown in Additional file 1: Figure S4. *, $P < 0.05$; **, $P < 0.01$.

spontaneously during DNA replication. A quantitative PCR (qPCR)-based assay demonstrated that treatment with 1.25–20 μM etoposide or bleomycin significantly increased the number of integrated viral DNA copies (Figure 4A). We performed a colony formation assay to further demonstrate the effects of DNA damaging agents on viral transduction. As shown in Figure 4B, treatment with DNA damaging agents significantly increased the number of drug-resistant colonies, indicating that DSBs promoted the integration of D64A virus (Figure 4B). In contrast, these compounds had no obvious effects on the integration of WT virus (Figure 4C and D). Although it has been reported that DSBs augment viral replication during multiple steps [15], our observations suggested that they enhance the integration step of viral DNA, which is a pivotal step in viral transduction.

DSB-dependent viral integration induced minor structural alterations in provirus DNA but generated infectious progeny viruses

It has been proposed that a non-homologous end-joining (NHEJ) pathway is involved in the repair of the gaps formed during viral integration [25] and that the DSB-specific integration of provirus DNA is susceptible to structural alterations [26]. To evaluate this, we quantified the frequency of structural modifications with provirus DNA using linear amplification mediated-PCR (LAM-PCR), followed by nucleotide sequence analysis [27]. When cells were infected with the virus in the presence of RAL, insertions and deletions in the 5′-LTR region were detected in 70.6% and 35.3% of cells, respectively (Table 1). In contrast, only 5% of the integrants were positive for structural alterations when infected in the presence of dimethyl sulfoxide (DMSO, solvent control) (Table 1 and Additional file 1: Figure S5). The data implicated that viral integration in the presence of RAL is susceptible to disruption of provirus DNA structures, which abrogated the production of secondary viruses.

To clarify this possibility, we investigated the effects of RAL on single-round viral infection using several cell lines. As shown in Figure 5A, we found that the infectivity of the WT virus was significantly attenuated by RAL, i.e., viral infection was reduced to 0.2% and 3.8% when 10 μM RAL was used to treat MAGIC5 cells and MT-4

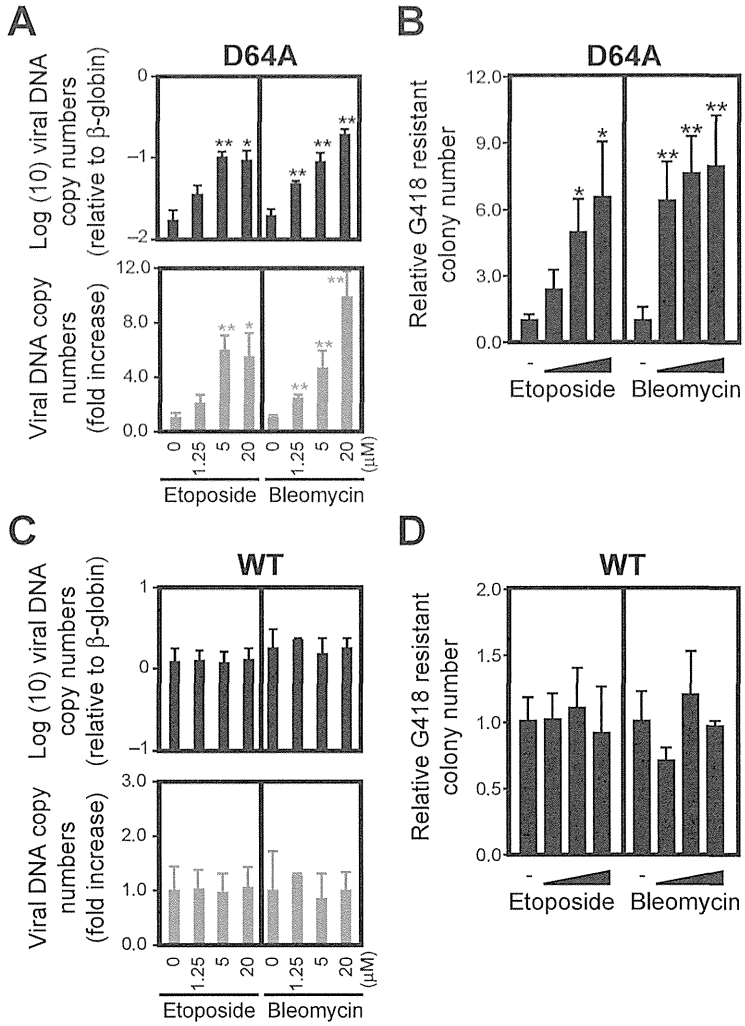

Figure 4 DNA damage enhances the integration rate of HIV-1. Serum-starved HT1080 cells were infected with D64A (**A**) or WT (**C**) viruses in the presence of etoposide or bleomycin from 0–24 hpi. After 48 h, genomic DNA was extracted and subjected to qPCR. Relative copy numbers of HIV-1 DNA to β-globin were estimated (top) and the fold increase of HIV-1 DNA copy number compared to control infection that was conducted without DNA damaging agents (bottom) were calculated. For colony formation assay, VSVG-pseudotyped D64A (NL-Neo-IN-D64A-E(−)R(−)) (**B**) or WT (NL-Neo-E(−)R(−)) (**D**) viruses, which had the neomycin resistant gene (Neo^R), were used. HT1080 cells were treated with various doses of etoposide or bleomycin for 24 h, which were added at the same time of viral infection. After selection with 600 μg/mL of G418, numbers of Neo^R colonies were counted. Numbers of Neo^R colonies were normalized by plating efficiency. Error bars, s.d. of triplicate assays. $^*P < 0.05$; $^{**}P < 0.01$.

cells, respectively. However, these values were the same with D64A virus, which suggests that restricting IN-CA could not block viral infection completely. This suggestion was supported by tests using azidothymidine (AZT, an RT inhibitor), which further blocked the infectivity of D64A virus. Importantly, the same results were obtained using elvitegravir (EVG, another IN-strand transfer inhibitor) in PMA-treated THP-1 cells (Figure 5A).

These observations strongly suggest that the WT virus can replicate in the presence of RAL, although the potential for viral replication is low and at similar level to IN-CA–defective virus. To test this possibility, we infected MT-4 cells with a replication-competent virus in the presence of RAL and examined the production of the progeny virus using MAGIC5 cells (HeLa/CD4, CCR5, LTR-β-gal) [28]. As shown in Figure 5B, we observed viral replication with the WT virus, although RAL was continuously added in the culture medium (one representative result from three independent experiments is shown with other experimental data in Additional file 1: Figure S6A). To exclude the possibility that the secondary virus possessed mutations that could overcome the inhibitory effects of RAL, we tested the viral RNA recovered from the culture supernatants. Analysis of the nucleotide sequences of 10

Table 1 HIV-1 DNA integration sites and host-virus junction sequence

Seq ID	Inhibitor	Chr	Locus	Strand	RefSeq gene	Insertion	Deletion
100902	DMSO	20	33371451	plus	NCOA6	-	-
100903	DMSO	17	35993714	minus	DDX52	-	-
100904	DMSO	3	156651874	minus	LEKR1	-	-
100906	DMSO	20	60900963	minus	LAMA5	-	-
100907	DMSO	3	19680267	minus	DLG1	-	-
100910	DMSO	4	150767744	plus	-	-	-
100912	DMSO	9	131400460	plus	WDR34	-	-
100914	DMSO	1	156020423	minus	UBQLN4	11bp (ACAGCAGTTAG)	37 bp
100916	DMSO	17	43551920	minus	PLEKHM1	-	-
100919	DMSO	20	2467413	minus	ZNF343	-	-
100921	DMSO	10	114725221	minus	TCF7L2	-	-
106501	DMSO	4	87017147	plus	MAPK10	-	-
106502	DMSO	2	98458616	minus	TMEM131	-	-
106505	DMSO	15	44399565	minus	FRMD10	-	-
106506	DMSO	2	197544261	plus	CCDC150	-	-
106510	DMSO	7	333212296	minus	BBS9	-	-
106513	DMSO	2	230499770	plus	DNER	-	-
106520	DMSO	17	38682989	plus	CR597260	-	-
106521	DMSO	19	17213409	minus	MY09B	-	-
106524	DMSO	6	33219360	plus	VPS52	-	-
100925	RAL	9	33033919	plus	DNAJA1	-	9 bp
100931	RAL	14	44024820	minus	-	-	20 bp
100937	RAL	2	102387409	plus	MAP4K4	9 bp (GACACTTAG0	-
100940	RAL	5	176735496	plus	MXD3	2 bp (AC)	-
100944	RAL	3	105267040	plus	-	21 bp (AATAAAAAGGTACAAATAGAC)	-
106525	RAL	14	87606685	minus	-	6 bp (TCATAA)	3 bp
106530	RAL	22	36006496	plus	MB	1 bp (A)	9 bp
106534	RAL	7	130544996	minus	CR618431	10 bp (TTGTAATTAC)	-
106537	RAL	1	63779999	minus	BC040309	16 bp (AAAGAAAAGGGGGGAC)	-
106538	RAL	3	190624485	minus	-	-	4 bp
106540	RAL	3	85084717	minus	CADM2	-	-
106542	RAL	18	40381428	minus	RIT2	2 bp (CA)	1 bp
106558	RAL	6	52427867	minus	TRAM2	-	-
106574	RAL	9	18460635	plus	-	9 bp (ACACCTAAT)	-
106582	RAL	1	6482403	minus	HES2	4 bp (GGAC)	-
106588	RAL	11	28954901	plus	-	4 bp (GGAC)	-
106596	RAL	7	92394729	plus	CDK6	4 bp (GGAC)	-

HIV-1 DNA integratio sites were determined by LAM-PCR. LAM-PCR sequence were aligned to the human genome reference (GRCh37/hg19, Feb. 2009, UCSC). Chr, chromosome.

progeny viruses revealed that all clones had no reported mutations related to RAL-resistant phenotypes (Table 2, Additional file 1, Table S1 and Figure S7) [29-32]. A similar experiment was performed using D64A virus. Again, we observed reproducible viral replication in the presence or absence of RAL (Figure 5C, Additional file 1: Figure S6B). Analysis of the nucleotide sequence of the progeny virus RNA revealed that a single clone of the 10 viruses analyzed was positive for a reported mutation linked to a RAL-resistant phenotype (M154I in Table 2, Additional file 1, Table S1). However, the other nine clones were free of such mutations. In addition, no WT virus revertants

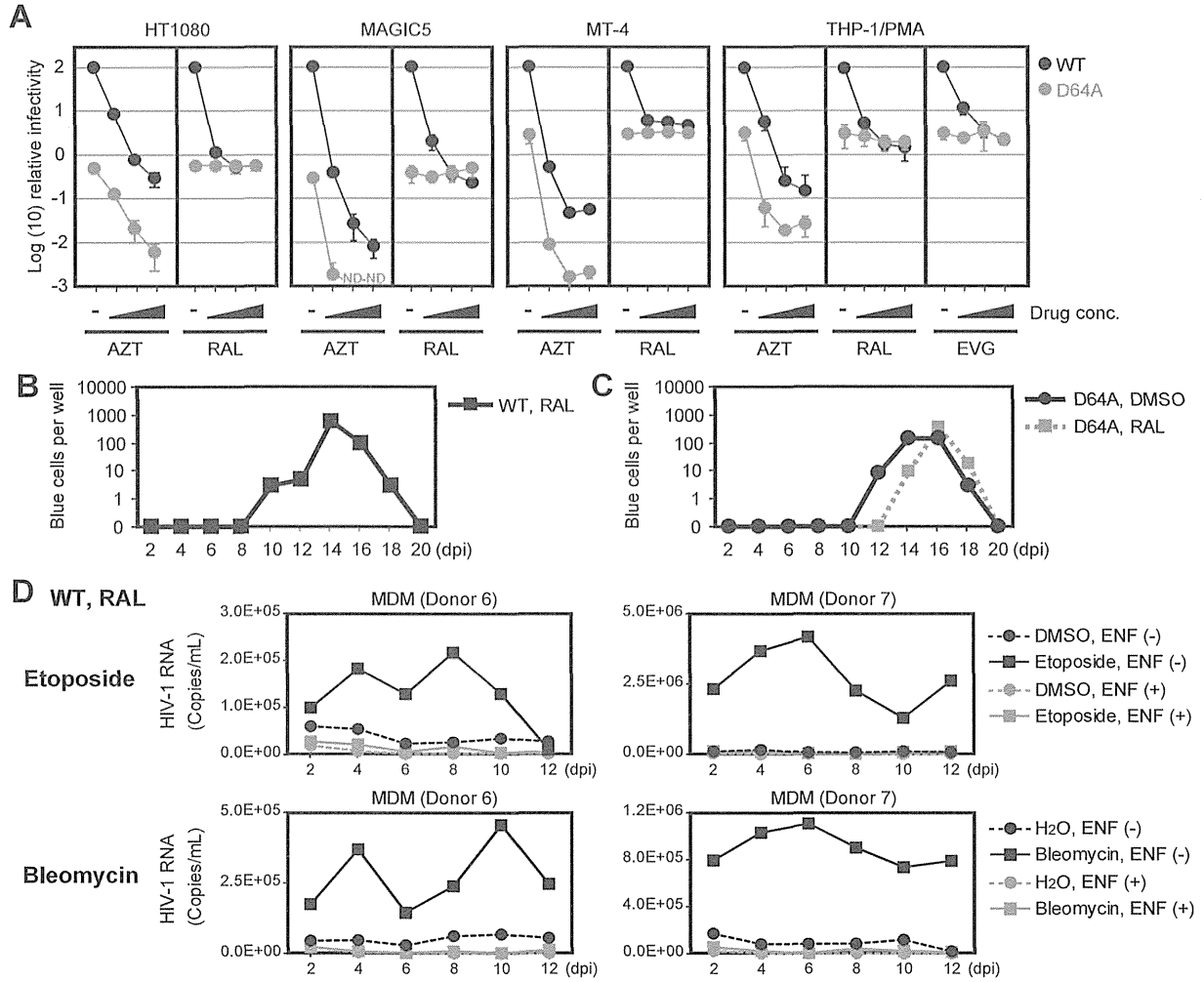

Figure 5 IN-CA deficient virus can produce infectious progeny virus. (**A**) Effect of RAL on the infectivity of WT and D64A viruses. After infection with VSVG-pseudotyped WT (NL-Luc-E(−)) or D64A (NL-Luc-IN-D64A-E(−)) virus in the presence of AZT, RAL or EVG, cells were harvested at 48 hpi and subjected to luciferase assay. Relative luciferase activity compared to a control sample, in which WT virus was infected without any compounds, were plotted. Concentration of AZT was 0, 1, 10 and 100 μM, whereas concentrations of RAL and EVG were 0, 0.1, 1 and 10 μM. Black circles, WT virus; gray circles, D64A virus; ND, not detected. Representative data of two independent experiments was shown. Error bars, s.d. of triplicate assays. (**B**) Functional evaluation of progeny viruses generated after IN-CA independent infection. MT-4 cells were infected in the presence of RAL with replication-competent WT virus (NL4-3). Then conditioned medium was harvested every 2 d, and infectivity of progeny virus present in the conditioned medium was evaluated using MAGIC5 cells. (**C**) Similar experiment with (**B**) was done using D64A (NL-IN-D64A) virus. Representative results of three independent experiments are shown. (**D**) Secondary virus generated from MDMs infected with virus in the presence of RAL. MDMs were infected with a replication-competent NL4-3 virus with an *env* gene, which was derived from R5-tropic ADA virus (NL-ADA-R(−)). Then, HIV-1 RNA copy number in the conditioned medium was quantified by RT-qPCR analysis. To evaluate effects of DNA damaging agents, 2.5 μM etoposide or 1.25 μM bleomycin were added from 0–2 dpi. To exclude the possibility that carry-over virions, which were remnant viruses that could not be completely removed after the initial infection, we included control sample, in which a fusion inhibitor enfuvirtide (ENF) was continuously added from 0 dpi to the end of assay.

were detected. It is interesting to note that MT-4, a cell line infected with human T cell leukemia virus, expresses Tax, a viral protein. One possible explanation for the efficient IN-CA independent viral infection is due to DNA damage that is induced by the biological activity of Tax [33,34].

After establishing that RAL-resistant viral replication could be induced in MT-4 cells, we investigated whether the same mode of viral infection can occur in MDMs. We detected no apparent replication of infectious secondary virus in MDMs, which were infected in the presence of RAL. However, viral replication was detected when DNA damaging agents were treated at the same time as the viral infection (Figure 5D). Importantly, the addition of enfuvirtide (ENF), a fusion inhibitor,

Table 2 IN mutations of NL-ADA or NL-IN-D64A-ADA viruses in Figure 5B and 5C

Virus	Clone #	RNA	Amino acid
WT/RAL	#1	-	-
	#5	-	-
	#6	-	-
	#7	-	-
	#8	-	-
	#9	-	-
	#10	-	-
	#2	A144G	E48E (Silent)
	#3	A87G	P29P (Silent)
	#4	A731G	R244K
D64A/ DMSO	#1	A191C	D64A
	#2	A191C	D64A
	#3	A191C	D64A
	#4	A191C	D64A
	#7	A191C	D64A
	#9	A191C	D64A
	#5	A191C, A772G	D64A, K258E
	#6	A191C, U842A	D64A, V281E
	#8	A38G, A191C, G462A	E13G, D64A, M154I
	#10	A191C, A279, A809G	D64A, T93T (Silent), D270G
D64A/RAL	#1	A191C	D64A
	#4	A191C	D64A
	#8	A191C	D64A
	#10	A191C	D64A
	#2	A191C, G806C	D64A, R269T
	#3	A191C, A718G	D64A, K240E
	#5	A191C, G829U	D64A, G277C
	#6	A191C, U598C	D54A, I200T
	#9	A191C, G462A	D64A, M154I
	#7	G7A, G39A, G103A, A191C	D3N, E13E (Silent), E35K, D64A

Nucleotide sequence of progeny viral RNA was analyzed. In two of 20 clones examined, we identified M1541, which was reported as a mutation related to RAL-resistant phenotype [30].

completely abolished the detection of the viral RNA, which indicated that the detected virus was not a remnant of the initially infected virus and that it was a progeny virus. Similar results were obtained in independent experiments using MDMs prepared from a different donor. These data and the absence of reported mutations in these viral RNA showed that DSBs promoted productive viral transduction even in the presence of RAL.

Based on these experiments, we expected that DSB site may capture and incorporate virus DNA as a structurally intact form. To obtain direct evidence for this possibility, we analyzed the nucleotide sequences of the provirus DNA integrated in the DSB site. In these experiments, serum-starved HT1080 cells were co-infected with an Ad-I-*Ppo*I and an IN-defective lentiviral vector (Lenti6-EGFP-D64V), which contained a blasticidin-resistant gene. After infection, the blasticidin-resistant cells were selected and cloned, and the lentivirus-infected cell clones were screened using I-*Ppo*I-qPCR. We isolated a total of 74 clones and obtained 10 (13.5%), five (6.8%), and five (6.8%) clones, which contained proviral DNA at the I-*Ppo*I site in direct, inverted, or both direct and inverted orientations, respectively (Figure 6A). Of these, five clones were EGFP-positive (Figure 6B) and the proviral DNA was integrated only into the I-*Ppo*I site in one of these clones (Figure 6C, D, clone #2413). This was further confirmed by fluorescent *in situ* hybridization (FISH) analysis, which detected provirus DNA in a single locus in the genome (Figure 6E). Sequence analysis of the provirus DNA of clone #2413 finally identified an intact viral DNA structure with the flanking nucleotide sequence of the I-*Ppo*I site (Figure 6F). The data indicated clearly that the structurally intact viral DNA could integrate into the DSB site.

Vpr mimicked DSBs and enhanced the IN-CA–independent viral transduction into resting macrophages

Vpr, an accessory gene of HIV-1, encodes a 96-amino acid virion-associated nuclear protein with pleiotropic activities, including a cell cycle abnormality during the G2/M phase, enhanced promoter activity and apoptosis. It has also been proposed that Vpr is important for macrophage infection through the nuclear trafficking of a preintegration complex [35]. Previously, it has been reported that Vpr elicits cellular signals triggered by DNA damage [36-40], which suggests that Vpr promotes IN-CA–independent viral transduction. To test this hypothesis, we checked whether infection with R+ virus induced the DNA damage response in MDMs (Figure 7A). In agreement with our previous observations, infection with R+ virus evoked the cellular response triggered by DNA damage [36,37,41,42]. We investigated the infectivity of R+ virus and observed that Vpr enhanced viral transduction in the presence of RAL, which was blocked by AZT (Figure 7B). Similar to the effect of DSBs, Vpr enhanced the viral infectivity during the integration step (Figure 7C). Moreover, Vpr enhanced the infection of MDMs by D64A virus (Figure 7D and Additional file 1: Figure S8).

To further elucidate the effects of Vpr on the infection of MDMs, we compared the efficiency of viral transduction

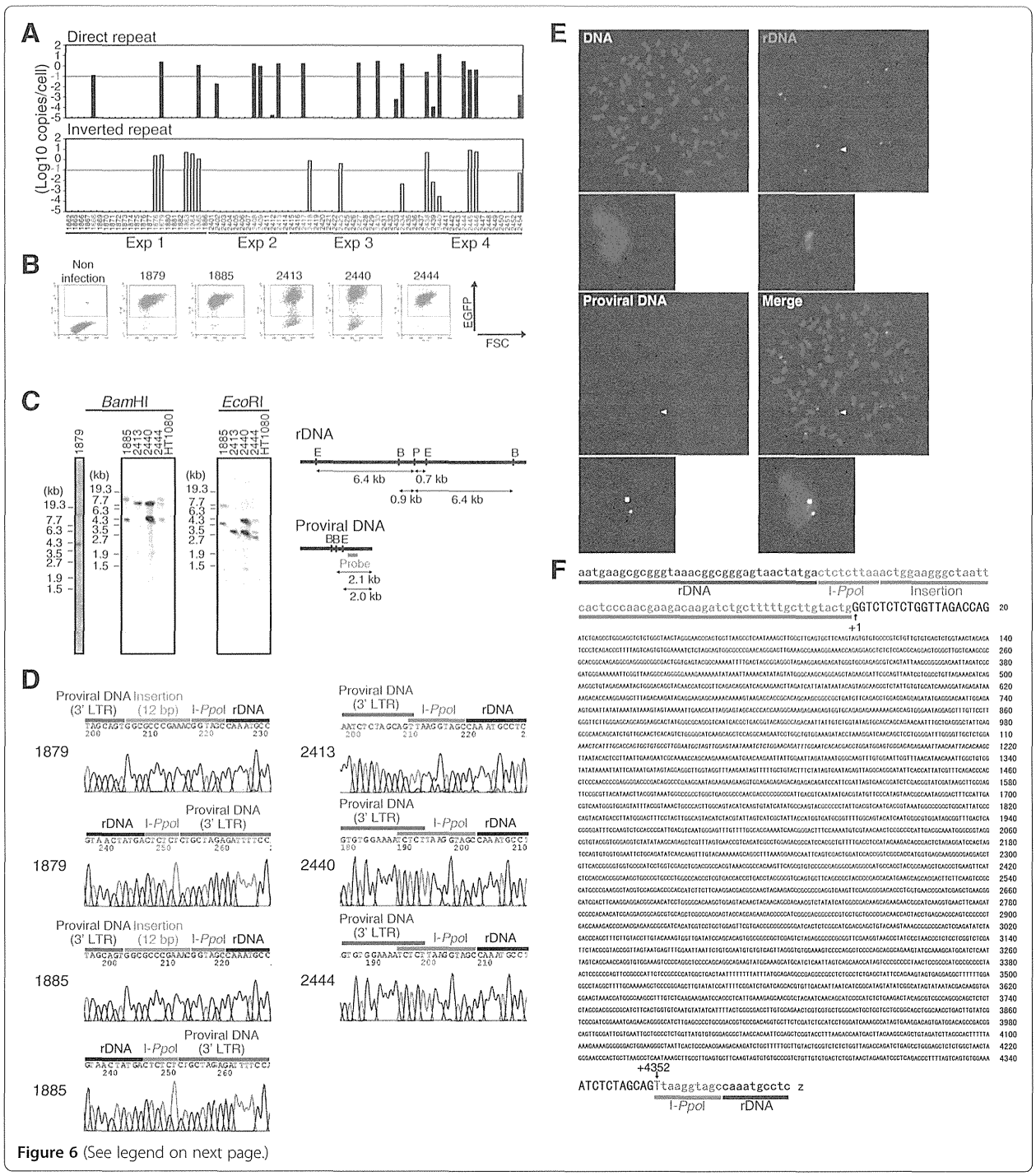

Figure 6 (See legend on next page.)

(See figure on previous page.)
Figure 6 Detection of intact provirus DNA in the DSB site. (**A**) I-*Ppo*I-qPCR screening of cell clones containing provirus DNA in I-*Ppo*I site. HT1080 cells were infected with Ad-I-*Ppo*I at an MOI of 30 in the medium with 0.1% FBS. After 24 h, cells were further infected with lentiviruses (VSVG-pseudotyped Lenti6-EGFP-D64V) also under serum-starved conditions. Two h later, medium was changed with fresh one with 0.1% FBS. On the next day, medium was replaced with a complete medium with 10% FBS. Blasticidin-resistant colonies were isolated and I-*Ppo*I site targeting provirus was detected by I-*Ppo*I-qPCR. The threshold of detecting provirus integrated as direct or inverted repeat orientation was −1 log(10) copies/cell (indicated in red horizontal lines). (**B**) EGFP expression analysis. Cells containing the proviral DNA in I-*Ppo*I site in (**A**) were further analyzed for the expression of EGFP by flow cytometer. (**C**) The estimation of proviral DNA copy number. Copy numbers of provirus DNA in EGFP-positive clones, shown in (**B**), were analyzed by Southern blot by using a part of DNA fragment of the lentiviral vector as a probe. Genomic DNA extracted from each clone was digested with *Bam*HI or *Eco*RI prior to electrophoresis. Restriction maps are shown (right panel). B, *Bam*HI; E, *Eco*RI; P, I-*Ppo*I. Of note, clone #2413 possessed a single copy of provirus DNA. (**D**) Sequence analysis of lentiviral vector integrated in the I-*Ppo*I site. EGFP-positive clones shown in (**B**) were subjected to sequence analysis. I-*Ppo*I-PCR amplicons were directly used as a template for sequence analysis. (**E**) FISH analysis of the #2413 clone. (**F**) Nucleotide sequence of intact proviral DNA present in the DSB site. The proviral DNA of #2413 clone was sequenced and whole nucleotide sequence data was shown. In #2413 clone, no structural alternations of provirus DNA were detected.

into MDMs, peripheral blood mononuclear cells (PBMCs), and human cell lines by calculating the fold-increase in the luciferase activity, which reflected the infectivity of each virus (Figure 7E, Additional file 1, Figure S9). As summarized in Figure 7F, the positive effects of Vpr were the most striking when MDMs were infected with D64A virus (D64A/R+ virus). The infectivity of D64A/R+ virus in MDMs was 37.0–265.1-fold higher than that of D64A/R− virus. In contrast, these positive effects were not detected with the WT/R+ virus. Moreover, the positive effects of Vpr were less conspicuous in PBMCs, consistent with previous observations that Vpr functions as a positive factor during viral transduction into MDMs [43]. Combined with previous reports that Vpr activates ATM [36,37] and ATR [38], our observations suggest that the enhanced infectivity of D64A/R+ virus in MDMs is attributable to Vpr-induced DSBs [36,37].

Discussion

Since it was first postulated that the cellular proteins responsible for DNA damage repair are positively involved in HIV-1 infection [9], roles of DSBs and DNA damage repair enzymes in viral infection have remained controversial [10-14,16-19,44]. However, several lines of evidence have suggested that DSBs have at least two roles in viral infectivity, i.e., direct upregulation of the rate of viral DNA integration into the host genome and the activation of DNA damage repair enzymes, which contribute to multiple steps in HIV-1 infection including repair of the gaps formed during the integration of viral DNA into the host genome [15]. Here we focused on the first possibility and provided experimental data, which showed that DNA damage increased the frequency of viral integration into the host genome.

In particular, we found that DSBs promoted the transduction of D64A virus, which was defective with respect to the catalytic activity of integrase (IN-CA). Moreover, DSBs upregulated the infectivity of WT virus by overcoming the inhibitory effects of RAL, an IN-CA inhibitor. Furthermore, infectious secondary viruses were generated from the provirus DNA formed through IN-CA–independent viral transduction. Our observations were highly consistent with previous reports that the IN-CA–defective virus can integrate into the host genome [45-47]. Ebina *et al.* reported that the integration rate of the IN-CA–defective virus was enhanced by DNA damaging agents such as x-ray irradiation or hydrogen peroxide [48], whereas we showed that DSBs upregulated IN-CA–independent viral integration and promoted the production of secondary viruses, which were competent for subsequent viral infection. Importantly, analysis of the nucleotide sequences of the viral RNA from the secondary viruses showed that there were no revertants to WT virus. Most of the viruses analyzed also had no reported mutations linked to RAL-resistant phenotypes [29-32]. Taken together with observation that RAL could reduce the infectivity of WT virus at a similar level to D64A virus, our data also suggest that currently available IN inhibitors cannot completely block productive viral infection, which is possibly enhanced by DSBs.

The mechanism of DSB-induced upregulation of viral transduction remains elusive but our data suggest that DSB sites provide a platform where viral DNA integrates in an IN-CA–independent manner. When cells were co-infected with HIV-1 virus and an adenovirus that expressed rare-cutting endonucleases such as I-*Sce*I or I-*Ppo*I, we reproducibly observed that the viral DNA was integrated into the corresponding DSB sites. However, interestingly, DSB-site specific viral integration was influenced by viral and cellular factors. First, we observed that targeting of viral DNA to the DSB site was observed mainly during IN-CA–independent viral transduction, although its frequency was low compared with WT virus. Second, it was influenced by the cellular conditions of the target cells, i.e., the frequency of IN-CA-independent viral transduction into DSB sites decreased from approximately 53% to 18% when the concentration of FBS was changed from 0.1% to 10% (Figure 2C). These results and the FACS analysis suggest that this difference may be because the spontaneous DSBs generated during DNA replication also captured viral

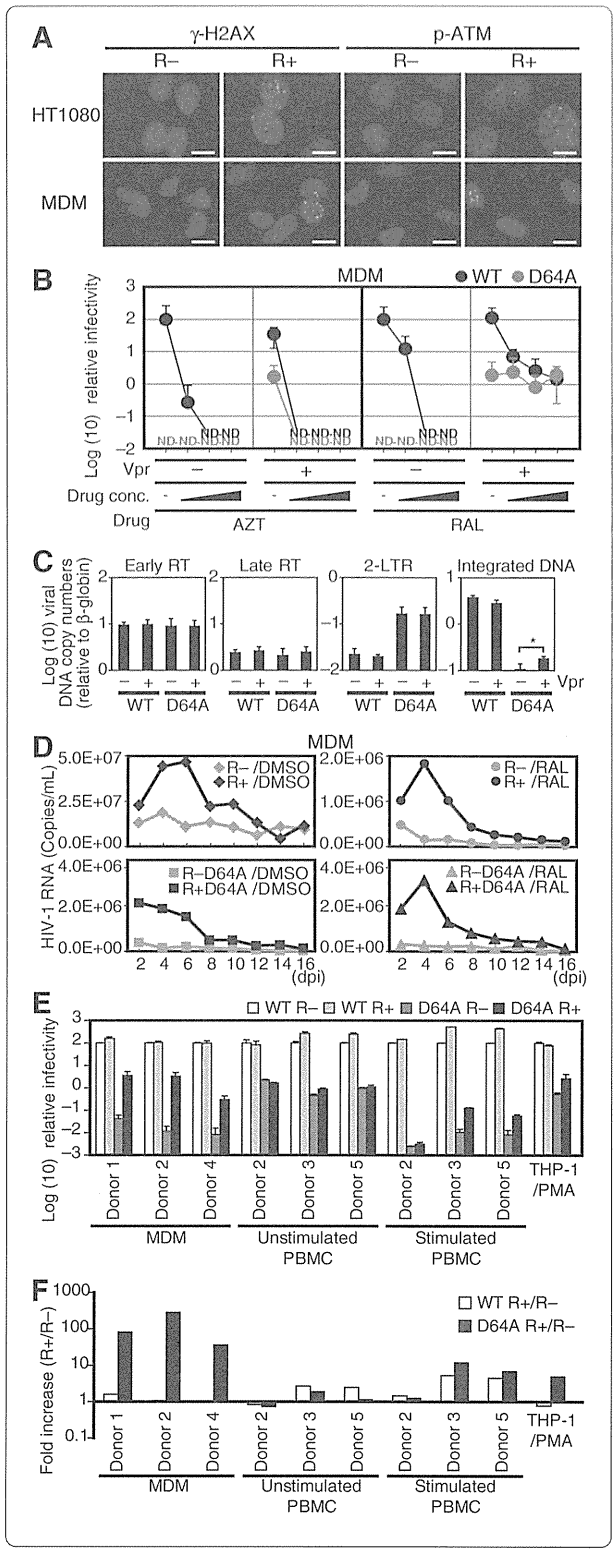

Figure 7 Vpr mimics DNA damaging agents, and enhances the IN-CA independent macrophage infection. (**A**) Vpr induces DNA damage cellular signals in MDMs. HT1080 cells or MDMs were infected with VSVG-pseudotyped R– virus (NL-Luc-E(–)R(–)) or R+ virus (NL-Luc-E(–)), and then analyzed immunochemically. Bars = 10 μm. (**B**) Effect of RAL on the infectivity of WT and D64A viruses. MDMs were infected with WT or D64A viruses in the presence of AZT or RAL. The cells were harvested at 48 hpi and subjected to luciferase assay. Relative luciferase activity values to WT R– infectivity are shown. Black circles, WT; gray circles, D64A; ND, not detected. Error bars, s.d. of triplicate assays. (**C**) Effects of Vpr on the integration of viral DNA into the host genome. Serum-starved HT1080 cells were infected with VSVG-pseudotyped IN WT or D64A mutant virus with or without Vpr. After 48 h, infected cells were subjected to qPCR analysis. Error bars, s.d. of triplicate assays. *$P < 0.05$. (**D**) HIV-1 replicates in MDMs in the presence of RAL. Replication-competent NL4-3 with an intact *env* gene derived from R5-tropic ADA viruses (NL-ADA, NL-ADA-R(–), NL-ADA-IN-D64A, and NL-ADA-IN-D64A-R(–)) were infected. Then, copy numbers of HIV-1 RNA in the conditioned medium was quantified by RT-qPCR. **E** and **F**) Positive effects of Vpr on infection of D64A virus into MDMs. Primary cells and cell lines were infected with IN WT or D64A mutant virus with or without Vpr. Cells were harvested at 48 hpi and subjected to luciferase assay. (**E**) Relative luciferase activity values to WT R– infectivity are shown. White bars, WT/R–; light gray bars, WT/R+; dark gray bars, D64A/R–; black bars, D64A/R+. Error bars, s.d. of triplicate assays. (**F**) Fold increase of R+ virus infectivity to R– virus. White bars, WT; black bars, D64A.

DNA, which resulted in a decrease in the relative rate of viral integration into artificially induced DSBs.

Interestingly, the DSB-specific integration of DNA fragments has been reported for hepatitis B virus DNA, an adeno-associated viral vector (AAV) [49,50], and Ty1 [51], a DNA retrotransposon of *Saccharomyces cerevisiae.* These observations suggest that the DSB site-specific integration of exogenous DNA fragments is not lentivirus-specific, which also indicates that DSB site-specific integration is dependent on the cellular response to DNA damage. We observed that KU55933, a specific ATM inhibitor, consistently blocked DSB-specific viral integration (Figures 1D and 2D). Interestingly, x-ray irradiation triggers the retrotransposition of long interspersed element 1 in human cells, which is also dependent on ATM [52], implying that a conserved cellular response to DNA damage is functionally involved in the capture of viral DNA in the DSB site.

We detected minor nucleotide deletions of approximately <9 bp in five of six clones of the provirus DNA, which were derived from cells infected with virus in the presence of RAL (Table 1). Such structural alternations would be due to the NHEJ repair system that is involved in viral integration in the presence of RAL. Because it has been reported that provirus DNA with 10-bp deletions from nucleotides +3 to +12 in the 5′-LTR remained functional [53], such provirus DNA is likely to be replication competent, although minor modifications in the 5′-LTR may be related to reduced expression of viral mRNA, as reported by Ebina *et al.* [48].

Several researchers have proposed that viral mRNA is expressed from non-integrated viral DNA of the IN-CA-defective virus [54,55], whereas Vpr was shown to promote *Nef* mRNA expression from such an extrachromosomal viral DNA [56]. However, our study clearly indicated that Vpr upregulates integration of IN-CA–defective virus into the host genome. The positive effects of Vpr on viral transduction were more prominent in MDMs than in PBMCs, well consistent with reports that Vpr functions as a positive factor during viral transduction into MDMs. Combined with observations that Vpr activates ATM [36,37] and ATR [38] and that macrophages are resistant to DSBs compared with monocytes [20], our data suggest that the enhancement of IN-CA–independent viral transduction into MDMs may be a pivotal role of Vpr in HIV-1 infection.

In summary, our observations may have major importance in the debate on the involvement of cellular factors in viral integration. It has been postulated that DNA damage sensor molecules are involved in the efficient integration of viral DNA. It has also been claimed that DNA damage sensor proteins have no involvement in DNA damage-dependent viral integration. Here we showed that DSBs are particularly important for IN-CA–independent viral transduction and that the effects of DSBs should be analyzed in carefully designed experimental conditions or else their effects are obscured. Collectively, our data suggest that complete prevention of viral integration will require the development of novel compounds that can protect cells from IN-CA–independent viral integration.

Conclusion

The ATM-dependent mode of the DSB-specific viral DNA integration and Vpr-induced DSBs may be novel targets for anti-HIV compounds that inhibit viral transduction into MDMs, which are a persistent focus of HIV-1 infection.

Methods

Plasmid constructs

The vesicular stomatitis virus glycoprotein (VSVG) expression vector pHIT/G [57], the HIV-1 proviral construct pNL4-3 [58], pNL-ADA [59], and the HIV-1 proviral indicator constructs pNL-Luc-E(−) and pNL-Luc-E(−)R(−) [37] have been described previously. To introduce D64A mutation into IN (adenine of nucleotide 4420 to cytosine) to create pNL-IN-D64A, site-directed mutagenesis (QuikChange; Stratagene) was performed using pNL4-3 as a template. To create pNL-ADA-IN-D64A and pNL-Luc-IN-D64A-E(−) that contained D64A mutants, the *Spe*I-*Pfl*MI fragment (nucleotides 1507–5297) of pNL-IN-D64A was replaced with those of pNL-ADA and pNL-Luc-E(−), respectively. To create the Vpr-deficient construct pNL-ADA-R(−), pNL-ADA-IN-D64A-R(−), and pNL-Luc-IN-D64A-E(−)R(−), the *Pfl*MI-*Sal*I fragment (nucleotides 5297–5785) of pNL-Luc-E(−)R(−) was replaced with those of pNL-ADA, pNL-ADA-IN-D64A, and pNL-Luc-IN-D64A-E(−), respectively.

The neomycin-resistant marker expressing vector pNL-Neo-E(−)R(−) was created by inserting a PCR-amplified neomycin-resistant gene into the *Not*I-*Xho*I site of pNL-Luc-E(−)R(−). To create a neomycin-resistant marker expressing D64A, the mutant pNL-Neo-IN-D64A-E(−)R(−) was created by the *Spe*I-*Pfl*MI fragment (nucleotides 1507–5297) of pNL-IN-D64A and replaced with that of pNL-Neo-E(−)R(−). To create pIRES2-EGFP-I-*Sce*I, a pIRES2-EGFP (Clontech)-based plasmid with an I-*Sce*I recognition site, a synthetic double-stranded oligonucleotide (I-*Sce*I-sense and I-*Sce*I-antisense oligonucleotides; see Additional file 1: Table S2) was inserted into the *Eco*RI and *Bam*HI sites of pIRES2-EGFP.

To make the adenoviral vector Ad-I-*Ppo*I, I-*Ppo*I cDNA was amplified from pBabe-HA-ER-I-*Ppo*I using the Adeno-*Ppo*I-*Dra*I-F and Adeno-*Ppo*I-*Dra*I-R primers (Additional file 1: Table S2) and cloned into the *Swa*I site of the pAxCALNLwtit2 cosmid vector (NIPPON GENE). To generate the EGFP-expressing lentiviral vector (pLenti6-EGFP), *EGFP* cDNA from pENTR1a-EGFP was cloned into pLenti6/V5-DEST (Invitrogen) using LR Clonase (Invitrogen). The IN D64V mutation of the gag/pol-expressing plasmid pLP1 (Invitrogen; pLP1-IN-D64V) was introduced using pLP1 as a template with site-directed mutagenesis (QuikChange; Stratagene).

Cell culture

THP-1, HT1080, HEK293, and HEK293T cell lines were obtained from the RIKEN Cell Bank. TIG-3 (primary human fibroblast cells) and MT-4 cells were obtained from the Health Science Research Resources Bank (Osaka, Japan). HT1080, HEK293, HEK293T, MAGIC5, and TIG-3 cells were maintained in Dulbecco's modified Eagle's medium (DMEM) supplemented with 10% fetal bovine serum (FBS). MT-4 cell was maintained in RPMI 1640 supplemented with 10% FBS. To obtain macrophage-like cells, THP-1 cells, maintained in Iscove's modified Dulbecco's medium supplemented with 10% FBS, were treated for 2 d with 5.0×10^{-8} M PMA. As described previously [60], PMA-treated THP-1 cells were positive for Mac-1, a specific marker of macrophages. Peripheral blood was derived from healthy donors who worked within the institute and gave informed consent. Experimental procedures were approved by the internal review board. PBMCs and MDMs were prepared and cultured as previously described [61]. MDMs were prepared from healthy volunteers who gave informed consents. The experimental protocol was approved by the internal review board.

HIV-1 and lentiviral vector preparation

The preparation and titration of replication-competent and VSVG-pseudotyped viruses are described elsewhere [36,37,62,63]. The lentiviral vectors were prepared using pLenti6-EGFP and the ViraPower Lentiviral Packaging Mix (Invitrogen) according to the manufacturer's protocol. Viral supernatants were centrifuged at 120 × *g* for 5 min, filtered through a 0.2-μm filter, and stored at −80°C. To exchange the medium for DMEM supplemented with 0.1% FBS, the viruses were ultracentrifuged at 86,000 × *g* for 1 h.

Quantitative PCR of provirus DNA

For the quantification of early RT, late RT, 2-LTR circle, and integrated DNA, qPCR was performed as described elsewhere [64,65]. Briefly, cells were harvested at 48 hpi, and genomic DNA was prepared by QuickGene (FujiFilm). For the quantification of early RT, late RT, and 2-LTR circle products, the primers and probe sets M667/AA55/R-U5, M667/M661/R-U5, and MH535/2-LTR-AS/NL4-3-U3 were used, respectively. TaqMan Universal PCR Master Mix with UNG (Applied Biosystems) and ABI7000 (Applied Biosystems) were used according to the manufacturer's instructions. For Alu-PCR (quantification of integrated DNA), the primer and probe sets first-Alu-F/first-Alu-R/first-gag-R and second-tag-R/2-LTR-S/probe-2 were used for the first and second rounds of qPCR, respectively. The amplification conditions for the first round of PCR, using AmpliTaq Gold 360 Master Mix (Applied Biosystems), were as follows: 95°C for 10 min, followed by 12 cycles at 95°C for 15 s, 60°C for 30 s, and 72°C for 10 min. The second round of qPCR was conducted using TaqMan Universal PCR Master Mix according to the manufacturer's instructions. To generate a standard curve for Alu-PCR, HEK293T cells (approximately one million cells) were infected with VSVG-pseudotyped NL-Luc-E(−)R(−) virus (200 ng p24), then harvested at 30 d post-infection (dpi), and genomic DNA was prepared. For the quantification of β-globin DNA copy numbers, the primer set globin-F/globin-R was used with SYBR *Premix ExTaq* (TaKaRa). Sequence information for primers and probes is listed in Additional file 1: Table S2.

Cleavage of I-*Sce*I and I-*Ppo*I sites

Ad-I-*Sce*I and Ad-LacZ were prepared as described previously [36]. PMA-treated THP-1 cells were infected with Ad-I-*Sce*I or Ad-LacZ at 1 h post–HIV-1 infection for 1 h at a multiplicity of infection (MOI) of 100. In Figure 1E–1H, HT1080 cells were transfected with plasmid DNA that encoded a chmeric protein of estrogen receptor-I-*Ppo*I (ER-I-*Ppo*I), and then 4-hydroxytamoxifen (4-OHT) was added to activate the endonuclease and induce DSB. The pAxCALNLwtit2 cosmid vector harboring I-*Ppo*I cDNA was digested with *Bsp*T104I and transduced into HEK293 cells to produce Ad-I-*Ppo*I. The adenoviral vector encoding Cre recombinase, AxCANCre (TaKaRa), was co-infected with Ad-I-*Ppo*I at an MOI of 30 to remove the floxed stuffer between the CAG promoter and I-*Ppo*I cDNA.

Quantification of the I-*Sce*I site specific viral integration

PMA-treated THP-1 cells were co-infected with WT virus and Ad-I-*Sce*I or Ad-LacZ, and then extracted genomic DNA was subjected to I-*Sce*I-qPCR analysis. I-*Sce*I site targeting integration rate of HIV-1 DNA was estimated by PCR amplification using primer sets pIRES2eGFP+543F/pNL4-3+9207R and pIRES2eGFP+574F/pNL4-3+98R+9173R for the first and second rounds of qPCR, respectively. The amplification conditions for the first round of PCR, using *ExTaq* polymerase (TaKaRa), were as follows: 30 cycles of 98°C for 10 s, 60°C for 30 s, and 72°C for 30 s. The second round of qPCR was conducted using SYBR *Premix ExTaq* polymerase (TaKaRa) according to the manufacturer's instructions. For the second round PCR template, 1/25 the volume of the first PCR amplicon was used. To prepare a standard sample for the I-*Sce*I-qPCR, the 5'-LTR DNA fragment of HIV-1 was amplified using the pNL4-3+9074F-*Sce*-RI and pNL4-3+9423R-*Bam*HI and cloned into the *Eco*RI and *Bam*HI sites of pIRES2-EGFP (pIRES2-EGFP-5'-LTR). Then, HT1080 cells were transfected with pIRES2-EGFP-5'-LTR and HT1080/pIRES2-EGFP-5'-LTR cell was obtained. By Southern blot and sequence analyses we confirmed that two copies of the DNA fragment of pIRES2-EGFP-5'-LTR vector were present in HT1080/pIRES2-EGFP-5'-LTR diploid cells. Sequence information for primers and probes is listed in Additional file 1: Table S2.

Quantification of the I-*Ppo*I site specific viral integration

Serum starved HT1080 cells were co-infected with Ad-I-*Ppo*I and lentiviruses, which were generated by pLenti6-EGFP or pLP1-IN-D64V. To estimate I-*Ppo*I site targeting or total integration of the lentiviral vector, I-*Ppo*I-qPCR or EGFP-qPCR was conducted using the TaqMan Universal PCR Master Mix (Applied Biosystems). For I-*Ppo*I-qPCR in the direct or inverted repeat orientation, the primer sets rDNA+11725R/pLenti6+5237F or rDNA+11645F/pLenti6+5237F were used, respectively; pLenti6-LTR was used as the TaqMan probe. For EGFP-qPCR, the primers EGFP-F/EGFP-R and TaqMan EGFP-probe were used. As a standard sample for estimating copy numbers of viral DNA integrated in the I-*Ppo*I site, genomic DNA of HT1080/Lenti6-EGFP-std cells were was used. We have confirmed by Southern blot and sequence analyses that HT1080/Lenti6-EGFP-std cells harbored two copies of Lenti6-EGFP proviral DNA in both orientations in the I-*Ppo*I site. On the other hand, as a standard sample for total provirus DNA, genomic DNA of HT1080/pIRES2-EGFP-5'-LTR cells, which possessed two copies of *EGFP*, were

used. Sequence information for primers and probes is listed in Additional file 1: Table S2.

PCR and sequence analysis

To amplify the host DNA/5'-LTR junction at the I-*Sce*I site, the primer sets pIRES2eGFP+543F/pNL4-3+9207R and pIRES2eGFP+574F/pNL4-3+98R+9173R were used for the first and second rounds of PCR, respectively. To amplify the host DNA/3'-LTR junction at the I-*Sce*I site, the primer sets pIRES2eGFP+1910R/L-M667 and pIRES2eGFP+887R/LambdaT were used for the first and second rounds of PCR, respectively. The amplification conditions for the host DNA/5'-LTR and host DNA/3'-LTR were as follows: 40 cycles for the first round of PCR or 30 cycles for the second round of PCR at 98°C for 10 s, 60°C for 30 s, and 72°C for 30 s and 35 cycles at 98°C for 10 s, 60°C for 30 s, and 72°C for 60 s for the first round of PCR and 30 s for the second round of PCR, respectively. *ExTaq* polymerase (TaKaRa) was used for the PCR. PCR amplicons were used directly or cloned into pCR2.1-TOPO (Invitrogen) as a template for sequence analysis. To amplify the rDNA/lentiviral vector at the I-*Ppo*I site in the direct repeat orientation, the primer sets rDNA+11784R/pLenti6+5208F and rDNA+11747R/pLenti6+5232F were used for the first and second rounds of PCR, respectively. To amplify the rDNA/lentiviral vector at the I-*Ppo*I site in the inverted repeat orientation, the primer sets rDNA+11589F/pLenti6+5208F and rDNA+11612F/pLenti6+5232F were used for the first and second rounds of PCR, respectively. The amplification conditions for the rDNA/lentiviral vector at the I-*Ppo*I site were as follows: 40 cycles for the first and second rounds of PCR at 98°C for 10 s, 60°C for 30 s, and 72°C for 30 s. *ExTaq* polymerase (TaKaRa) was used for PCR. PCR amplicons were used directly or cloned into pCR2.1-TOPO (Invitrogen) as a template for sequence analysis. To analyze the IN mutations of NL-ADA and NL-IN-D64A-ADA viruses in Figure 5B and 5C, viral RNAs were isolated from conditioned medium (14 dpi; WT/RAL and D64A/DMSO, 16 dpi; D64A/RAL) and amplified by primer set pNL+4207F/pNL+5120R and Titan One-Tube RT-PCR Kit (Roche diagnostics). The amplicons were cloned into pCR2.1-TOPO and sequenced. The primers are listed in Additional file 1: Table S2.

LAM-PCR

To estimate the rate of insertion and/or deletion, the LAM-PCR method was performed as described previously [27,66]. Briefly, 1.0×10^6 HT1080 cells were infected with VSVG-pseudotyped NL-Neo-E(−)R(−) virus (200 ng p24) in the presence of RAL or DMSO, and G418-resistant cells were harvested at 28 dpi and subjected to LAM-PCR. The sequence information for primers is listed in Additional file 1: Table S2.

Replication assay

To evaluate the production of functional virion from RAL-treated cells, 1×10^5 MT-4 cells were infected with replication-competent NL4-3 or NL-IN-D64A (20 ng p24). After 2 h of the infection, cells were washed with phosphate buffered saline (PBS) twice and suspended in 1.0 mL of medium. To prepare the culture supernatant, three-quarter of the cultures were harvested every 2 d, and the culture was continued by adding 750 μL of the complete medium into each well. From −1 dpi to harvest, MT-4 cells were treated with 10 μM RAL or DMSO. Conditioned medium (100 μL) was added to 1×10^4 MAGIC5 cells [28], and at 48 hpi, cells were stained by X-gal to estimate the number of transduced cells. To estimate HIV-1 RNA copy numbers, 1×10^5 MDMs were infected with NL-ADA, NL-ADA-R(−), NL-ADA-IN-D64A, or NL-ADA-IN-D64A-R(−) (20 ng p24) for 2 h, then washed with medium four times. Three-quarters of the conditioned medium was harvested and replaced with fresh medium every 2 d. From −1 dpi to harvest, MDMs were treated with 10 μM RAL or DMSO. HIV-1 RNA of conditioned medium was purified and subjected to RT-qPCR using the Lenti-X qRT-PCR Titration Kit (TaKaRa). To evaluate the effect of DNA damaging agents, 2.5 μM etoposide or 1.25 μM bleomycin were added to MDMs from 0–2 dpi. To exclude a possibility that detected HIV RNA merely reflect the RNA from carry-over virion, fusion inhibitor ENF, dissolved in phosphate buffer saline PBS, was added from 0 hpi to harvest as a negative control.

Colony formation assay

To evaluate the effect of DNA damaging agents on the integration rate of D64A mutant virus, serum-starved HT1080 cells (5×10^5 cells) in DMEM with 0.1% FBS were infected with a neomycin-resistant marker expressing VSVG-pseudotyped NL-Neo-IN-D64A-E(−)R(−) virus (100 ng p24) in the presence of 0 (DMSO), 0.625, 1.25, or 2.5 μM etoposide and 0 (water), 0.313, 0.625, or 1.25 μM bleomycin. Cells were selected with G418 from 2 dpi, then stained with Giemsa at 12 dpi. The G418-resistant colony numbers were normalized by plating efficiency, which represented the cytotoxicity of etoposide and bleomycin. The plating efficiencies after treatment of etoposide and bleomycin at 0, 0.625, 1.25, 2.5 μM were 100, 57.2, 26.0 and 19.5%, and 100, 60.4, 68.8 and 60.4%, respectively.

Immunohistochemical analysis

Detection of phosphorylated histone H2AX (γH2AX) and phosphorylated ATM (pATM) was done, according to the reported method using antibodies against γH2AX (phosphorylated at Ser 139, Millipore, cat no. 05–636) and pATM (Ser 1981, Millipore, cat. no. 05–740) [37].

Briefly, the cells were washed with PBS and fixed with 4% paraformaldehyde in PBS. The fixed cells were permeabilized with 0.2% Triton X-100 in PBS. After treatment with PBS supplemented with 10% goat serum for 30 min, the cells were incubated with antibodies. After 1 h of incubation at 37°C, secondary antibodies conjugated with Alexa 546 (Molecular Probes) were added for 1 h at 37°C. Nuclei were stained by Hoechst33258.

Luciferase assay

To evaluate the infectivity of viruses, 1.0×10^4 cells were infected with VSVG-pseudotyped luciferase viruses (2 ng p24) for 48 h, then subjected to luciferase assay by using One-Glo (Promega) and a Veritas Microplate luminometer (TURNER BIOSYSTEMS).

Flow cytometry

To analyze the status of cell cycle, HT1080 cells were labeled with 5 μM BrdU for 30 min and fixed in ice-cold 70% ethanol. Anti-BrdU-fluorescein (Roche Diagnostics) was used to stain the BrdU-labeled cells, according to the manufacturer's instructions. BrdU-labeled cells were analyzed by BD FACSCalibur flow cytometer (BD Biosciences). To analyze the percentages of EGFP-positive cells, Flow cytometry analysis was performed using a BD FACSCalibur.

FISH analysis

Metaphase FISH analysis was performed to estimate the proviral DNA copy number and co-localization of proviral DNA and rDNA using lentiviral vector and rDNA specific probes (Chromosome Science Labo Inc.).

Statistical analysis

Statistical significance was determined by Student's *t*-test, and values of $P < 0.05$ were considered statistically significant.

Additional file

Additional file 1: Figure S1. Southern blot analysis to verify the cleavage of the I-*Sce*I and I-*Ppo*I site. **Figure S2.** A schematic of the strand transfer of HIV-1 DNA to genomic DNA. **Figure S3.** Evaluation of lentiviral infectivity and cell cycle status of serum starved HT1080 cells by BrdU incorportion. **Figure S4.** Raw data in Figure 3. **Figure S5.** The percentage of insertion and/or deletion (InDel) mutations at the host/viral junction. **Figure S6.** Two additional independent data sets in Figure 5B and 5C. **Figure S7.** RAL in 2d cultured conditioned medium is active. **Figure S8.** Additinoal data sets with another donor in Figure 7D. **Figure S9.** Raw data in Figure 7E. **Table S1.** RAL and EVG resistant mutations reported in literature. **Table S2.** List of primers and probes used in this study. **Supplementary methods.** Southern blot analysis.

Competing interests

The authors declare no competing financial interests.

Authors' contributions

TK and BS designed and performed the work, analyzed the data and wrote the paper. KT and MT contributed reagents and technical advice for the work, and edited the manuscript. YI conceived of the study and supervised the work and wrote the paper. All authors read and approved the final manuscript.

Acknowledgements

We thank Dr. F. Graham (McMaster University, Canada) for the I-*Sce*I adenovirus vector, Dr. I. Saito (Tokyo University, Japan) for AxCALac8, Dr. M. O'Connor (KuDOS Pharmaceuticals, England) for KU55933, and Dr. M. B. Kastan (Duke Cancer Institute, USA) for pBABE-HA-ER-I-*Ppo*I. This work was supported by a Grant-in-Aid for Research on HIV/AIDS from the Ministry of Health, Labor, and Welfare of Japan.

Author details

[1]Department of Intractable Diseases, National Center for Global Health and Medicine, 1-21-1 Toyama, Shinjuku-ku, Tokyo 162-8655, Japan. [2]Research Group of HIV Molecular Epidemiology and Virology, The State Key Laboratory of Virology, Wuhan Institution of Virology, Chinese Academy of Sciences, Wuhan, Hubei 430071, China. [3]Department of Pathology, National Institute of Infectious Diseases, 1-23-1 Toyama, Shinjuku-ku, Tokyo 162-8640, Japan. [4]AIDS Research Center, National Institute of Infectious Diseases, 1-23-1 Toyama, Shinjuku-ku, Tokyo 162-8640, Japan.

Received: 26 June 2012 Accepted: 11 February 2013
Published: 21 February 2013

References

1. Perelson AS, Essunger P, Cao Y, Vesanen M, Hurley A, Saksela K, Markowitz M, Ho DD: **Decay characteristics of HIV-1-infected compartments during combination therapy.** *Nature* 1997, **387**:188–191.
2. Richman DD, Margolis DM, Delaney M, Greene WC, Hazuda D, Pomerantz RJ: **The challenge of finding a cure for HIV infection.** *Science* 2009, **323**:1304–1307.
3. Hazuda DJ, Felock P, Witmer M, Wolfe A, Stillmock K, Grobler JA, Espeseth A, Gabryelski L, Schleif W, Blau C, Miller MD: **Inhibitors of strand transfer that prevent integration and inhibit HIV-1 replication in cells.** *Science* 2000, **287**:646–650.
4. Dorr P, Westby M, Dobbs S, Griffin P, Irvine B, Macartney M, Mori J, Rickett G, Smith-Burchnell C, Napier C, *et al*: **Maraviroc (UK-427,857), a potent, orally bioavailable, and selective small-molecule inhibitor of chemokine receptor CCR5 with broad-spectrum anti-human immunodeficiency virus type 1 activity.** *Antimicrob Agents Chemother* 2005, **49**:4721–4732.
5. Jager S, Cimermancic P, Gulbahce N, Johnson JR, McGovern KE, Clarke SC, Shales M, Mercenne G, Pache L, Li K, *et al*: **Global landscape of HIV-human protein complexes.** *Nature* 2012, **481**:365–370.
6. Engelman A, Mizuuchi K, Craigie R: **HIV-1 DNA integration: mechanism of viral DNA cleavage and DNA strand transfer.** *Cell* 1991, **67**:1211–1221.
7. Engelman A, Craigie R: **Identification of conserved amino acid residues critical for human immunodeficiency virus type 1 integrase function in vitro.** *J Virol* 1992, **66**:6361–6369.
8. Brin E, Yi J, Skalka AM, Leis J: **Modeling the late steps in HIV-1 retroviral integrase-catalyzed DNA integration.** *J Biol Chem* 2000, **275**:39287–39295.
9. Daniel R, Katz RA, Skalka AM: **A role for DNA-PK in retroviral DNA integration.** *Science* 1999, **284**:644–647.
10. Smith JA, Wang FX, Zhang H, Wu KJ, Williams KJ, Daniel R: **Evidence that the Nijmegen breakage syndrome protein, an early sensor of double-strand DNA breaks (DSB), is involved in HIV-1 post-integration repair by recruiting the ataxia telangiectasia-mutated kinase in a process similar to, but distinct from, cellular DSB repair.** *Virol J* 2008, **5**:11.
11. Kameoka M, Nukuzuma S, Itaya A, Tanaka Y, Ota K, Ikuta K, Yoshihara K: **RNA interference directed against Poly(ADP-Ribose) polymerase 1 efficiently suppresses human immunodeficiency virus type 1 replication in human cells.** *J Virol* 2004, **78**:8931–8934.
12. Daniel R, Marusich E, Argyris E, Zhao RY, Skalka AM, Pomerantz RJ: **Caffeine inhibits human immunodeficiency virus type 1 transduction of nondividing cells.** *J Virol* 2005, **79**:2058–2065.
13. Daniel R, Katz RA, Merkel G, Hittle JC, Yen TJ, Skalka AM: **Wortmannin potentiates integrase-mediated killing of lymphocytes and reduces the efficiency of stable transduction by retroviruses.** *Mol Cell Biol* 2001, **21**:1164–1172.

14. Lau A, Swinbank KM, Ahmed PS, Taylor DL, Jackson SP, Smith GC, O'Connor MJ: **Suppression of HIV-1 infection by a small molecule inhibitor of the ATM kinase.** *Nat Cell Biol* 2005, **7**:493–500.
15. Sakurai Y, Komatsu K, Agematsu K, Matsuoka M: **DNA double strand break repair enzymes function at multiple steps in retroviral infection.** *Retrovirology* 2009, **6**:114.
16. Siva AC, Bushman F: **Poly(ADP-ribose) polymerase 1 is not strictly required for infection of murine cells by retroviruses.** *J Virol* 2002, **76**:11904–11910.
17. Dehart JL, Andersen JL, Zimmerman ES, Ardon O, An DS, Blackett J, Kim B, Planelles V: **The ataxia telangiectasia-mutated and Rad3-related protein is dispensable for retroviral integration.** *J Virol* 2005, **79**:1389–1396.
18. Baekelandt V, Claeys A, Cherepanov P, De Clercq E, De Strooper B, Nuttin B, Debyser Z: **DNA-Dependent protein kinase is not required for efficient lentivirus integration.** *J Virol* 2000, **74**:11278–11285.
19. Ariumi Y, Turelli P, Masutani M, Trono D: **DNA damage sensors ATM, ATR, DNA-PKcs, and PARP-1 are dispensable for human immunodeficiency virus type 1 integration.** *J Virol* 2005, **79**:2973–2978.
20. Bauer M, Goldstein M, Christmann M, Becker H, Heylmann D, Kaina B: **Human monocytes are severely impaired in base and DNA double-strand break repair that renders them vulnerable to oxidative stress.** *Proc Natl Acad Sci USA* 2011, **108**:21105–21110.
21. Tsuchiya S, Kobayashi Y, Goto Y, Okumura H, Nakae S, Konno T, Tada K: **Induction of maturation in cultured human monocytic leukemia cells by a phorbol diester.** *Cancer Res* 1982, **42**:1530–1536.
22. Anglana M, Bacchetti S: **Construction of a recombinant adenovirus for efficient delivery of the I-SceI yeast endonuclease to human cells and its application in the in vivo cleavage of chromosomes to expose new potential telomeres.** *Nucleic Acids Res* 1999, **27**:4276–4281.
23. Berkovich E, Monnat RJ Jr, Kastan MB: **Roles of ATM and NBS1 in chromatin structure modulation and DNA double-strand break repair.** *Nat Cell Biol* 2007, **9**:683–690.
24. Matsuo M, Kaji K, Utakoji T, Hosoda K: **Ploidy of human embryonic fibroblasts during in vitro aging.** *J Gerontol* 1982, **37**:33–37.
25. Skalka AM, Katz RA: **Retroviral DNA integration and the DNA damage response.** *Cell Death Differ* 2005, **12**(Suppl 1):971–978.
26. Perez EE, Wang J, Miller JC, Jouvenot Y, Kim KA, Liu O, Wang N, Lee G, Bartsevich VV, Lee YL, *et al*: **Establishment of HIV-1 resistance in CD4+ T cells by genome editing using zinc-finger nucleases.** *Nat Biotechnol* 2008, **26**:808–816.
27. Schmidt M, Schwarzwaelder K, Bartholomae C, Zaoui K, Ball C, Pilz I, Braun S, Glimm H, von Kalle C: **High-resolution insertion-site analysis by linear amplification-mediated PCR (LAM-PCR).** *Nat Methods* 2007, **4**:1051–1057.
28. Mochizuki N, Otsuka N, Matsuo K, Shiino T, Kojima A, Kurata T, Sakai K, Yamamoto N, Isomura S, Dhole TN, *et al*: **An infectious DNA clone of HIV type 1 subtype C.** *AIDS Res Hum Retroviruses* 1999, **15**:1321–1324.
29. McColl DJ, Chen X: **Strand transfer inhibitors of HIV-1 integrase: bringing IN a new era of antiretroviral therapy.** *Antiviral Res* 2010, **85**:101–118.
30. Mouscadet JF, Delelis O, Marcelin AG, Tchertanov L: **Resistance to HIV-1 integrase inhibitors: a structural perspective.** *Drug Resist Updat* 2010, **13**:139–150.
31. Serrao E, Odde S, Ramkumar K, Neamati N: **Raltegravir, elvitegravir, and metoogravir: the birth of "me-too" HIV-1 integrase inhibitors.** *Retrovirology* 2009, **6**:25.
32. Shafer RW, Schapiro JM: **HIV-1 drug resistance mutations: an updated framework for the second decade of HAART.** *AIDS Rev* 2008, **10**:67–84.
33. Baydoun HH, Bai XT, Shelton S, Nicot C: **HTLV-I tax increases genetic instability by inducing DNA double strand breaks during DNA replication and switching repair to NHEJ.** *PLoS One* 2012, **7**:e42226.
34. Matsuoka M, Jeang KT: **Human T-cell leukemia virus type 1 (HTLV-1) and leukemic transformation: viral infectivity, Tax.** *HBZ and therapy. Oncogene* 2011, **30**:1379–1389.
35. Malim MH, Emerman M: **HIV-1 accessory proteins–ensuring viral survival in a hostile environment.** *Cell Host Microbe* 2008, **3**:388–398.
36. Nakai-Murakami C, Shimura M, Kinomoto M, Takizawa Y, Tokunaga K, Taguchi T, Hoshino S, Miyagawa K, Sata T, Kurumizaka H, *et al*: **HIV-1 Vpr induces ATM-dependent cellular signal with enhanced homologous recombination.** *Oncogene* 2007, **26**:477–486.
37. Tachiwana H, Shimura M, Nakai-Murakami C, Tokunaga K, Takizawa Y, Sata T, Kurumizaka H, Ishizaka Y: **HIV-1 Vpr induces DNA double-strand breaks.** *Cancer Res* 2006, **66**:627–631.
38. Roshal M, Kim B, Zhu Y, Nghiem P, Planelles V: **Activation of the ATR-mediated DNA damage response by the HIV-1 viral protein R.** *J Biol Chem* 2003, **278**:25879–25886.
39. Daniel R, Kao G, Taganov K, Greger JG, Favorova O, Merkel G, Yen TJ, Katz RA, Skalka AM: **Evidence that the retroviral DNA integration process triggers an ATR-dependent DNA damage response.** *Proc Natl Acad Sci USA* 2003, **100**:4778–4783.
40. Belzile JP, Richard J, Rougeau N, Xiao Y, Cohen EA: **HIV-1 Vpr induces the K48-linked polyubiquitination and proteasomal degradation of target cellular proteins to activate ATR and promote G2 arrest.** *J Virol* 2010, **84**:3320–3330.
41. Nakai-Murakami C, Minemoto Y, Ishizaka Y: **Vpr-induced DNA double-strand breaks: molecular mechanism and biological relevance.** *Curr HIV Res* 2009, **7**:109–113.
42. Taneichi D, Iijima K, Doi A, Koyama T, Minemoto Y, Tokunaga K, Shimura M, Kano S, Ishizaka Y: **Identification of SNF2h, a chromatin-remodeling factor, as a novel binding protein of Vpr of human immunodeficiency virus type 1.** *J Neuroimmune Pharmacol* 2011, **6**:177–187.
43. Connor RI, Chen BK, Choe S, Landau NR: **Vpr is required for efficient replication of human immunodeficiency virus type-1 in mononuclear phagocytes.** *Virology* 1995, **206**:935–944.
44. Smith JA, Daniel R: **Up-regulation of HIV-1 transduction in nondividing cells by double-strand DNA break-inducing agents.** *Biotechnol Lett* 2011, **33**:243–252.
45. Leavitt AD, Robles G, Alesandro N, Varmus HE: **Human immunodeficiency virus type 1 integrase mutants retain in vitro integrase activity yet fail to integrate viral DNA efficiently during infection.** *J Virol* 1996, **70**:721–728.
46. Nakajima N, Lu R, Engelman A: **Human immunodeficiency virus type 1 replication in the absence of integrase-mediated dna recombination: definition of permissive and nonpermissive T-cell lines.** *J Virol* 2001, **75**:7944–7955.
47. Gaur M, Leavitt AD: **Mutations in the human immunodeficiency virus type 1 integrase D, D(35)E motif do not eliminate provirus formation.** *J Virol* 1998, **72**:4678–4685.
48. Ebina H, Kanemura Y, Suzuki Y, Urata K, Misawa N, Koyanagi Y: **Integrase-independent HIV-1 infection is augmented under conditions of DNA damage and produces a viral reservoir.** *Virology* 2012, **427**:44–50.
49. Miller DG, Petek LM, Russell DW: **Adeno-associated virus vectors integrate at chromosome breakage sites.** *Nat Genet* 2004, **36**:767–773.
50. Bill CA, Summers J: **Genomic DNA double-strand breaks are targets for hepadnaviral DNA integration.** *Proc Natl Acad Sci USA* 2004, **101**:11135–11140.
51. Moore JK, Haber JE: **Capture of retrotransposon DNA at the sites of chromosomal double-strand breaks.** *Nature* 1996, **383**:644–646.
52. Farkash EA, Kao GD, Horman SR, Prak ET: **Gamma radiation increases endonuclease-dependent L1 retrotransposition in a cultured cell assay.** *Nucleic Acids Res* 2006, **34**:1196–1204.
53. Masuda T, Planelles V, Krogstad P, Chen IS: **Genetic analysis of human immunodeficiency virus type 1 integrase and the U3 att site: unusual phenotype of mutants in the zinc finger-like domain.** *J Virol* 1995, **69**:6687–6696.
54. Wu Y, Marsh JW: **Selective transcription and modulation of resting T cell activity by preintegrated HIV DNA.** *Science* 2001, **293**:1503–1506.
55. Engelman A, Englund G, Orenstein JM, Martin MA, Craigie R: **Multiple effects of mutations in human immunodeficiency virus type 1 integrase on viral replication.** *J Virol* 1995, **69**:2729–2736.
56. Poon B, Chang MA, Chen IS: **Vpr is required for efficient Nef expression from unintegrated human immunodeficiency virus type 1 DNA.** *J Virol* 2007, **81**:10515–10523.
57. Fouchier RA, Meyer BE, Simon JH, Fischer U, Malim MH: **HIV-1 infection of non-dividing cells: evidence that the amino-terminal basic region of the viral matrix protein is important for Gag processing but not for post-entry nuclear import.** *EMBO J* 1997, **16**:4531–4539.
58. Adachi A, Gendelman HE, Koenig S, Folks T, Willey R, Rabson A, Martin MA: **Production of acquired immunodeficiency syndrome-associated retrovirus in human and nonhuman cells transfected with an infectious molecular clone.** *J Virol* 1986, **59**:284–291.
59. Tokunaga K, Greenberg ML, Morse MA, Cumming RI, Lyerly HK, Cullen BR: **Molecular basis for cell tropism of CXCR4-dependent human immunodeficiency virus type 1 isolates.** *J Virol* 2001, **75**:6776–6785.
60. Mizoguchi I, Ooe Y, Hoshino S, Shimura M, Kasahara T, Kano S, Ohta T, Takaku F, Nakayama Y, Ishizaka Y: **Improved gene expression in resting macrophages using an oligopeptide derived from Vpr of human**

immunodeficiency virus type-1. *Biochem Biophys Res Commun* 2005, 338:1499–1506.
61. Hoshino S, Konishi M, Mori M, Shimura M, Nishitani C, Kuroki Y, Koyanagi Y, Kano S, Itabe H, Ishizaka Y: **HIV-1 Vpr induces TLR4/MyD88-mediated IL-6 production and reactivates viral production from latency.** *J Leukoc Biol* 2010, 87:1133–1143.
62. Iwabu Y, Fujita H, Kinomoto M, Kaneko K, Ishizaka Y, Tanaka Y, Sata T, Tokunaga K: **HIV-1 accessory protein Vpu internalizes cell-surface BST-2 /tetherin through transmembrane interactions leading to lysosomes.** *J Biol Chem* 2009, 284:35060–35072.
63. Iwabu Y, Kinomoto M, Tatsumi M, Fujita H, Shimura M, Tanaka Y, Ishizaka Y, Nolan D, Mallal S, Sata T, Tokunaga K: **Differential anti-APOBEC3G activity of HIV-1 Vif proteins derived from different subtypes.** *J Biol Chem* 2010, 285:35350–35358.
64. Butler SL, Hansen MS, Bushman FD: **A quantitative assay for HIV DNA integration in vivo.** *Nat Med* 2001, 7:631–634.
65. Yamamoto N, Tanaka C, Wu Y, Chang MO, Inagaki Y, Saito Y, Naito T, Ogasawara H, Sekigawa I, Hayashida Y: **Analysis of human immunodeficiency virus type 1 integration by using a specific, sensitive and quantitative assay based on real-time polymerase chain reaction.** *Virus Genes* 2006, 32:105–113.
66. Schmidt M, Zickler P, Hoffmann G, Haas S, Wissler M, Muessig A, Tisdale JF, Kuramoto K, Andrews RG, Wu T, *et al*: **Polyclonal long-term repopulating stem cell clones in a primate model.** *Blood* 2002, 100:2737–2743.

doi:10.1186/1742-4690-10-21
Cite this article as: Koyama *et al.*: DNA damage enhances integration of HIV-1 into macrophages by overcoming integrase inhibition. *Retrovirology* 2013 10:21.

ELSEVIER

Institut Pasteur

Microbes and Infection 15 (2013) 280–290

www.elsevier.com/locate/micinf

Original article

Characteristics of IFITM, the newly identified IFN-inducible anti-HIV-1 family proteins

Nopporn Chutiwitoonchai [a], Masateru Hiyoshi [a], Yuka Hiyoshi-Yoshidomi [a], Michihiro Hashimoto [a], Kenzo Tokunaga [b], Shinya Suzu [a,*]

[a] *Center for AIDS Research, Kumamoto University, Honjo 2-2-1, Chuo-ku, Kumamoto-city, Kumamoto 860-0811, Japan*
[b] *Department of Pathology, National Institute of Infectious Diseases, Tokyo 162-8640, Japan*

Received 19 July 2012; accepted 10 December 2012
Available online 30 January 2013

Abstract

IFN-inducible IFITM proteins (IFITM1, 2, and 3) inhibit the replication of various viruses including HIV-1 through poorly understood mechanisms. Here, we further analyzed characteristics of these newly identified HIV-1 restriction factors. Firstly, in contrast to other anti-HIV-1 proteins, such as tetherin and APOBEC3G, IFITMs were resistant to a down-regulation of surface expression or degradation by HIV-1 proteins. Secondly, the enforced expression of IFITMs reduced the production of HIV-1 viruses from cells transfected with proviral plasmids containing whole viral sequences. Although their inhibitory activities were modest when compared to that of tetherin, IFITMs, but not tetherin, directly reduced the expression of HIV-1 proteins including Gag, Vif and Nef. Of importance, however, IFITMs had no inhibitory effect when these viral proteins were expressed by codon-optimized cDNAs that bypassed the viral-specific expression machinery. Indeed, our results supported the idea that IFITMs interfere with viral protein expression mediated by double-stranded viral RNAs, such as RRE and TAR. Finally, the S-palmitoylation of IFITMs, which is crucial for their anti-influenza virus activity, was not required for their anti-HIV-1 activity, indicating that IFITMs restrict these viruses at different steps. These characteristics lead to a better understanding of the mechanism by which IFITMs restrict HIV-1 and other viruses.

Keywords: IFITM; Tetherin; APOBEC3G; HIV-1; IFN; Antiviral activity

1. Introduction

Type I interferons (IFN) are cytokines of the innate immune system that induce the expression of antiviral proteins upon viral infection. Viral recognition induces the activation of cellular signaling pathways that trigger the production of IFN, which leads to the expression of a set of IFN-stimulated genes that inhibit viral replication through diverse mechanisms [1,2]. The IFN-induced transmembrane (IFITM) genes were identified as IFN-stimulated genes [3]. Among this family of proteins, IFITM1, 2, and 3 are ubiquitously expressed. Although it has been reported that IFITM1 and IFITM3 play distinct roles in mouse primordial germ cell homing and repulsion [4], their precise physiological functions remain largely unknown. Intriguingly, recent studies have revealed that IFITM family proteins are potent inhibitors of influenza virus, West Nile virus, dengue virus [5–8], Marburg and Ebola filoviruses, SARS coronavirus [9], vesicular stomatitis virus [10], HCV [11], and HIV-1 [12,13]. However, it remains unclear how these small proteins, which are composed of approximately 130 amino acids, exert antiviral activity against a broad range of viruses.

Recently, Lu et al. showed that the knockdown of all three *ifitm* genes increased the susceptibility of TZM-bl HeLa cells to HIV-1 infection [12]. Consistent with this result, the enforced expression of IFITM1, 2, or 3 markedly suppressed HIV-1 replication in SupT1 T cells without affecting cell proliferation, the cell cycle, or the cell surface expression of

* Corresponding author. Tel.: +81 96 373 6828; fax: +81 96 373 6825.
E-mail address: ssuzu06@kumamoto-u.ac.jp (S. Suzu).

1286-4579/$ - see front matter © 2013 Institut Pasteur. Published by Elsevier Masson SAS. All rights reserved.
http://dx.doi.org/10.1016/j.micinf.2012.12.003

the HIV-1 entry receptor CD4 [12]. Schoggins et al. also reported that the enforced expression of IFITM2 or 3 had a similar inhibitory effect on HIV-1 replication using another T cell line, MT-4 [13]. Although HIV-1 entry step was clearly inhibited by IFITM2 and 3, the entry step might not be the primary target of IFITM1 during its restriction of HIV-1 replication, since IFITM1 did not affect HIV-1 entry but efficiently suppressed HIV-1 replication in SupT1 cells [12]. Indeed, it was shown that the intracellular region, rather than the N- or C-terminal extracellular domains, of IFITM1 is required for its inhibitory effect on HIV-1 [12]. Importantly, Lu et al. also showed that the enforced expression of IFITMs led to a reduction in the expression of the structural HIV-1 protein Gag, which might be simply due to the reduced viral replication. Nevertheless, it is also possible that IFITMs directly affect Gag expression.

In addition to the mechanism by which they suppress Gag expression, there are several unanswered questions regarding IFITMs. HIV-1 encodes proteins that antagonize the activities of IFN-inducible antiviral proteins. For instance, tetherin (also known as BST-2 or CD317) blocks the release of nascent virions from infected cells, but the HIV-1 accessory protein Vpu acts as a viral antagonist by inducing the down-regulation of tetherin expression at the cell surface [14–19]. Similarly, the cytidine deaminase APOBEC3G, whose expression is elevated by IFN [20], causes the hyper-mutation of HIV-1 cDNA, but another HIV-1 accessory protein, Vif, antagonizes its anti-HIV-1 activity by inducing the degradation of APOBEC3G [21–27]. However, it has not been examined whether HIV-1 antagonizes the anti-HIV-1 activity of IFITMs. Curiously, in contrast to the findings of two independent studies [12,13], Neil et al. failed to observe an inhibitory effect of the enforced expression of IFITMs on HIV-1 production in a study in which they identified tetherin as an HIV-1 restriction factor [15]. In this study, we therefore attempted to investigate whether HIV-1 proteins affect the expression and localization of IFITMs, how anti-HIV-1 activity of IFITMs and tetherin are different, and how IFITMs affect the expression of HIV-1 proteins in order to further understand the characteristics of these newly identified HIV-1 restriction factors.

2. Materials and methods

2.1. IFITM and tetherin plasmids

The N-terminal Flag-tagged human IFITM1, 2, and 3 cDNAs were provided by Liang [12], and subcloned into the pcDNA3.1 vector (Invitrogen). It was shown that IFITM3 was S-palmitoylated at three membrane-proximal cysteine residues (C71, C72, and C105) [7]. We therefore prepared three different mutants of Flag-tagged IFITM3, in which these cysteines had been mutated (singly or in combination) to alanine (C1/2A, C3A, and C1/2/3A; see Fig. 6A for details). As these cysteines are conserved in IFITM2 (C70, C71, and C104), similar mutants of IFITM2 were also prepared. The mutants were prepared using the QuikChange II Site-Directed Mutagenesis Kit (Stratagene) and appropriate mutagenic primers and cloned into the pcDNA3.1 vector. The nucleotide sequences of the mutants were verified using the BigDye Terminator v3.1 Cycle Sequencing Kit and an ABI PRISM 3100 Genetic Analyzer (Applied Biosystems). Extracellular Flag-tagged human tetherin (BST-2-exFlag) cloned into the pCAGGS vector was prepared as described previously [28].

2.2. HIV-1 plasmids

A proviral NL43 plasmid and a *vpu*-deleted mutant version of the plasmid (pNL-uE65) were provided by Adachi [29]. A proviral JRFL plasmid in which the *nef* gene had been replaced with that of the SF2 strain was prepared as described previously [30]. A codon-optimized Gag–GFP fusion expression plasmid (synGag–GFP) cloned into the pcDNA3.1 vector (Ohmine et al., manuscript under review) was kindly provided by Y. Ikeda (Mayo Clinic, Rochester, MN). Codon-optimized Vpu (Vphu) and Vif (HVif) expression plasmids cloned into the pcDNA3.1 vector were obtained through the NIH AIDS Research and Reference Reagent Program (Division of AIDS, National Institute of Allergy and Infectious Diseases, National Institutes of Health, Bethesda, MD), both of which were derived from the NL43 strain [31]. Two different Nef (the SF2 strain) expression plasmids were prepared as described previously [32,33]: Nef fused to the C-terminus of the extracellular/transmembrane regions of CD8 (CD8-Nef) was cloned into the pRc/CMV vector and Nef fused to the N-terminus of GFP (Nef–GFP) was cloned into the pAcGFP-N1 vector (Clontech). The NL43 strain Rev expression plasmid cloned into the pCAGGS vector was prepared as described previously [28]. In this study, we also created Gag and Gag/Pol expression plasmids (pCA-Gag-RRE and pCA-GagPol-RRE, respectively) by inserting PCR-amplified NL43-derived *gag* and *gag/pol* genes (nucleotides 790–2292 and 790–5096, respectively) together with a Rev-response element (RRE; nucleotides 7759–7992) into the pCAGGS vector.

2.3. Transfection

HEK293 cells (Invitrogen) were maintained in DME medium (Wako, Osaka, Japan) supplemented with 10% FCS (Nichirei Biosciences, Tokyo, Japan). The cells were seeded onto 12-well tissue culture plates at a density of 1.8×10^5 cells/well and transfected with various plasmids using 4 μl/well Lipofectamine 2000 reagent (Invitrogen), as described previously [30,32]. The total amount (1.6 μg/well) of the plasmid was normalized using appropriate control (empty) vectors. After 6 h of transfection, the culture medium was replaced with fresh medium, and the cells were cultured for an additional 42 h and then subjected to p24 Gag protein ELISA, Western blotting, flow cytometric analysis, or immunofluorescence analysis. In another experiment (see Fig. 5), the double-stranded RNA-dependent protein kinase (PKR) inhibitor C16 (imidazolo-oxindole; Sigma) was added to the culture (0.1% v/v) during the changing of the medium. The inhibitor was dissolved in DMSO (Wako), and the same volume of DMSO was used as a vehicle control.

2.4. p24 Gag ELISA

Viral production was assessed by measuring the concentration of p24 Gag protein in the culture supernatant [30]. The supernatants of the transfected 293 cells were clarified by brief centrifugation, and their p24 concentrations were analyzed by ELISA (ZeptoMetrix, Buffalo, NY). The absorbance of each well was measured at 450 nm with a microplate reader (Bio-Rad Laboratories).

2.5. Western blotting

The preparation of the total cell lysates and Western blotting was performed essentially as described previously [34]. Briefly, the cells were lysed on ice for 30 min with Nonidet P-40 lysis buffer (1% Nonidet P-40, 50 mM Tris, and 150 mM NaCl) containing protease inhibitors (1 mM EDTA, 1 μM PMSF, 1 μg/ml aprotinin, 1 μg/ml leupeptin, and 1 μg/ml pepstatin). The cell lysates were centrifuged and the resultant supernatants were resolved by SDS-polyacrylamide gel electrophoresis (SDS-PAGE) under reducing conditions. The proteins were transferred to a nylon membrane (Hybond-P; GE Healthcare). The antibodies used were as follows: anti-Gag (#65-004; Bio-Academia, Osaka, Japan), anti-Nef (#2949; NIH AIDS Research and Reference Reagent Program), anti-Vif (#319; NIH AIDS Research and Reference Reagent Program), anti-GFP (#FL; Santa Cruz Biotechnology), anti-Flag (clone M2; Sigma), and anti-actin (#C-2; Santa Cruz Biotechnology). The detection was performed with HRP-labeled secondary antibodies (anti-rabbit or anti-mouse IgG; GE Healthcare), the Immunostar LD Western blotting detection reagent (Wako), and an image analyzer (ImageQuant LAS 4000; GE Healthcare).

2.6. Flow cytometry

The cell surface expression of the Flag-tagged IFITM or Flag-tagged tetherin was assessed by the flow cytometric analysis, essentially as described previously [35]. The transfected 293 cells were detached using the enzyme-free cell dissociation buffer (Gibco), stained on ice for 30 min with PE-labeled anti-Flag antibody (60 μg/ml; Columbia Biosciences, Columbia, MD), and analyzed using a FACSCalibur (Becton Dickinson) and Cell Quest Software (Becton Dickinson). In a selected experiment (see Fig. 2C), 293 cells stably expressing human CD4 [32] were transfected and analyzed for the cell surface expression of CD4 using PE-labeled anti-CD4 antibody (clone RPA-T4, eBioscience).

2.7. Immunofluorescence

For immunostaining, the transfected 293 cells were directly fixed in 2% paraformaldehyde, permeabilized with 0.2% Triton X-100, and stained with the primary antibodies for 12 h followed by labeled secondary antibodies [32,33]. The following primary antibodies were used: anti-Flag (clone M2; Sigma, to detect Flag-tagged IFITM proteins) and anti-Gag (#65-004; BioAcademia). Anti-mouse IgG-AlexaFluor488 and anti-rabbit IgG-AlexaFluor568 (both from Molecular Probes) were used as the labeled secondary antibodies. Nuclei were stained with DAPI (Molecular Probes), and fluorescent signals were visualized with a BZ-8000 fluorescent microscope (Keyence, Osaka, Japan) equipped with Plan-Fluor ELWD 20×/0.45 objective lenses (Nikon). Image processing was performed using a BZ-analyzer (Keyence) and the Adobe Photoshop software (Adobe Systems).

2.8. Statistical analysis

The statistical significance of differences between samples was determined using the Student's *t*-test. *p* Values less than 0.05 were considered significant.

3. Results and discussion

3.1. IFITM3 and tetherin restrict HIV-1 at different steps

It has been shown that the knockdown of IFITMs increases the susceptibility of TZM-bl HeLa cells to HIV-1 infection and that their enforced expression suppresses HIV-1 replication and Gag expression in SupT1 cells [12]. However, in a study in which the enforced expression of tetherin was found to strongly inhibit viral release from 293 cells, IFITMs failed to display a similar inhibitory effect [15]. Therefore, we initially compared their anti-HIV-1 activities in the same system, i.e., the co-transfection into 293 cells. Viral production was monitored by assessing the concentration of p24 Gag protein in the culture supernatants. In this study, we found that IFITM3 significantly reduced viral production when it was co-transfected with the proviral NL43 plasmid containing the whole viral sequence (Fig. 1A, left graph). A similar inhibitory effect was also observed when IFITM3 was co-transfected with the *vpu*-deleted NL43 mutant (NL43-ΔVpu; right graph). When analyzed using the TZM-bl reporter cells, the infectivity of the WT viruses produced in the presence of IFITM3 was comparable to that of the control viruses (data not shown). Tetherin also reduced viral production, but its inhibitory effect was more marked when it was co-transfected with NL43-ΔVpu (Fig. 1A). This was due to the ability of Vpu to down-regulate the cell surface expression of tetherin [14–19]. In the experiment shown in Fig. 1A, we used 0.6 μg IFITM3 expression plasmid. When the same amount of plasmid was used, tetherin displayed a lower expression level (Fig. 1B) but stronger inhibitory activity (Fig. 1A) than IFITM3. These results indicated that the inhibitory effect of IFITM3 on viral production is modest when compared with that of tetherin, which explains why Neil et al. [15] failed to observe an inhibitory effect of IFITMs in their study. The importance was that IFITM3 and tetherin restricted HIV-1 at different steps because IFITM3 but not tetherin significantly reduced the expression levels of the p55 and p24 Gag proteins in the cells (Fig. 1C). It therefore appears that tetherin inhibits the release of viruses without affecting intracellular Gag expression whereas IFITM3 directly reduces intracellular Gag expression, and thereby suppresses viral production.

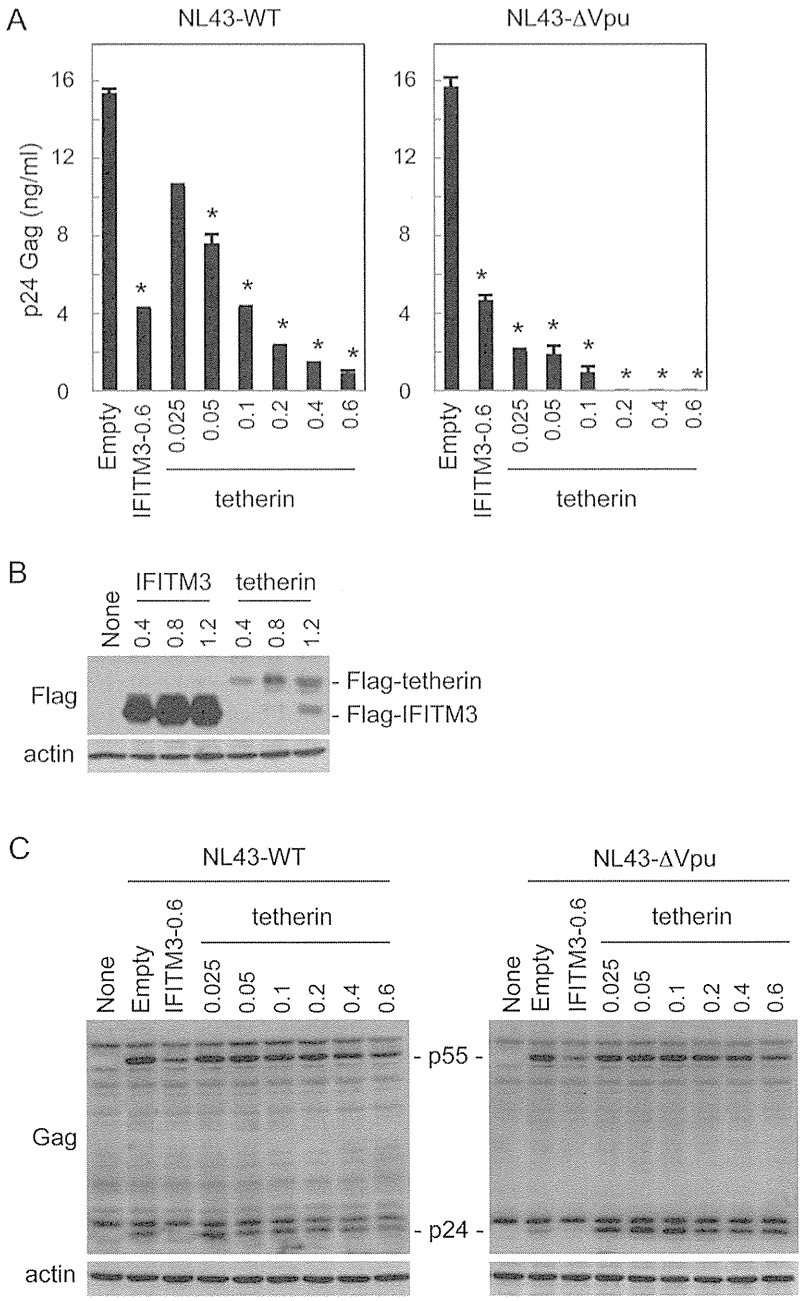

Fig. 1. The effects of IFITM3 and tetherin on viral production and Gag expression. (A) The 293 cells were transfected with the wild-type (NL43-WT, 0.6 μg) or *vpu*-deleted NL43 proviral plasmid (NL43-ΔVpu, 0.6 μg), or co-transfected with the empty vector (Empty, 0.6 μg), the IFITM3 expression plasmid (0.6 μg), or the indicated amount (0.025–0.6 μg) of the tetherin expression plasmid. The cells were cultured for 2 days, and the p24 Gag concentrations in the culture supernatants were determined by ELISA. Data are shown as the mean ± SD of triplicate assays and are representative of two independent experiments with similar results. $^{*}p < 0.05$. (B) The 293 cells were transfected with the empty vector (None), or the indicated amount (0.4, 0.8, or 1.2 μg) of the IFITM3 or tetherin expression plasmid, lysed after being cultured for 2 days, and analyzed for the expression of Flag-tagged IFITM3 or tetherin by Western blotting using anti-Flag antibody. The actin blot is a loading control. (C) The 293 cells were transfected as described in panel A, lysed after being cultured for 2 days, and analyzed for the expression of p55 and p24 Gag by Western blotting using anti-Gag antibody. The actin blot is a loading control. Data shown are representative of two independent experiments with similar results.

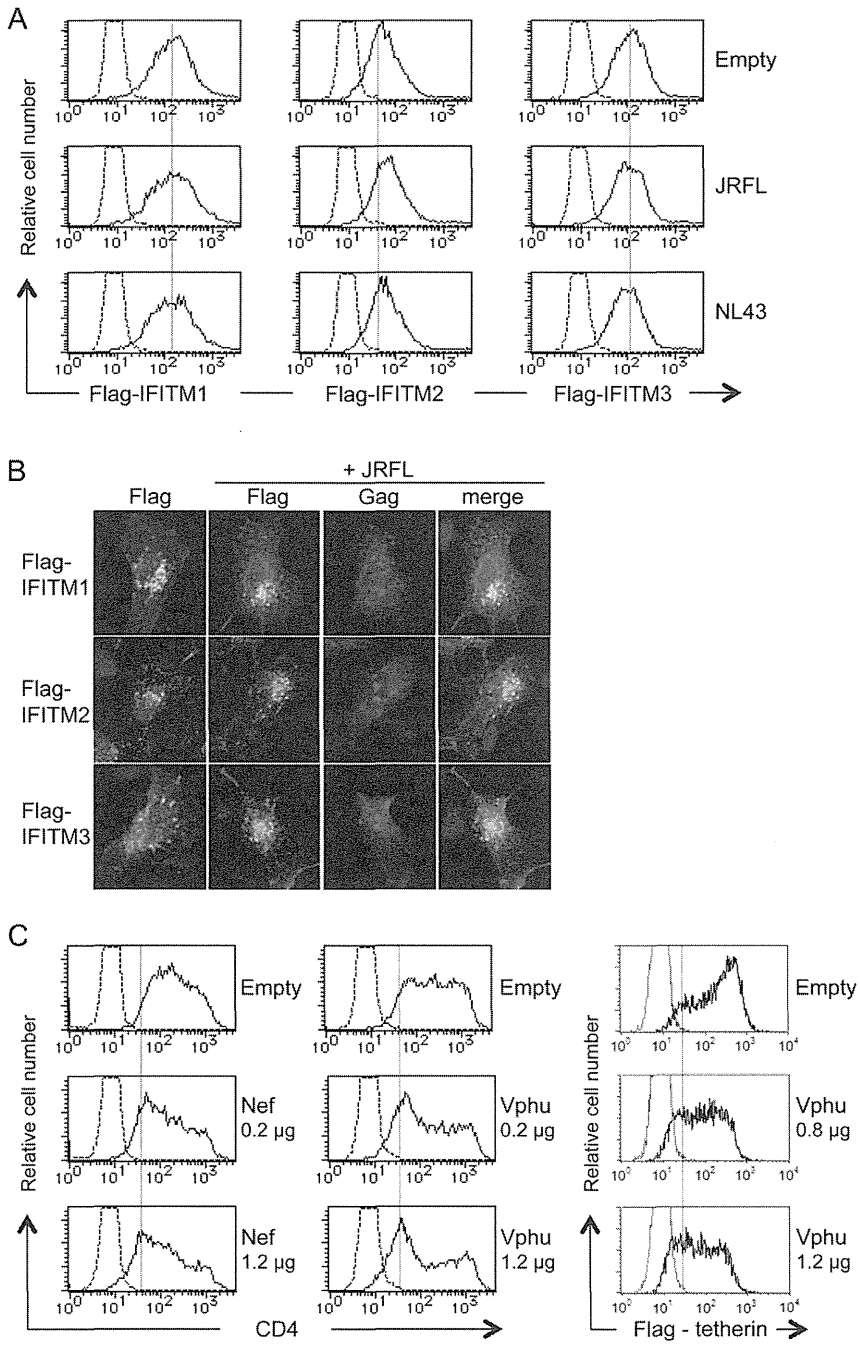

Fig. 2. The effects of HIV-1 proteins on the cell surface expression and intracellular distribution of IFITMs. (A) The 293 cells were co-transfected with the Flag-tagged IFITM1, -2, or -3 expression plasmid (0.4 μg) and the following plasmids (1.2 μg): the empty vector (Empty), the proviral NL43 plasmid, or the JRFL plasmid. The cells were cultured for 2 days, detached from the wells using the enzyme-free cell dissociation buffer, and analyzed for the cell surface expression of Flag-tagged IFITMs by flow cytometry using PE-labeled anti-Flag antibody. Data shown are representative of two independent experiments with similar results. (B) The 293 cells were transfected with the Flag-tagged IFITM1, 2, or 3 expression plasmid alone (0.4 μg) or co-transfected with the proviral JRFL plasmid (1.2 μg), cultured for 2 days, and co-stained with anti-Flag antibody (green), anti-Gag antibody (red), and DAPI (blue). (C) The 293 cells stably expressing human CD4 were transfected with the empty vector (Empty), the CD8-Nef fusion expression plasmid (0.2 or 1.2 μg), or the codon-optimized Vpu expression plasmid (Vphu, 0.2 or 1.2 μg). The cells were analyzed as in panel (A) using PE-labeled anti-CD4 antibody. Alternatively, 293 cells were co-transfected with Flag-tagged tetherin expression plasmid (0.4 μg) and the following plasmids: the empty vector (Empty, 1.2 μg) or the codon-optimized Vpu expression plasmid (Vphu, 0.8 or 1.2 μg). The cells were cultured for 2 days and analyzed as in panel (A). (For interpretation of the references to colour in this figure legend, the reader is referred to the web version of this article.)